5.4 Evaporator and absorber

Liquid ammonia from the condenser (8) enters the evaporator to cause refrigerating effect. Liquid ammonia is evaporated under low partial pressure in an atmosphere of an auxiliary gas, helium. The evaporated ammonia vapor is absorbed by the strong solution. It is initially assumed that liquid ammonia could be totally evaporated and absorbed. Then, the obtained refrigerating capacity could be determined from

$$\dot{Q}_{evap} = \dot{m}_8 X_8 (h_{12-vap} - h_8)$$
 (5.14)

The state 12-vap is considered as the evaporated ammonia after producing refrigerating effect. It is considered that only ammonia is evaporated. Therefore, the amount of water in the evaporator remains constant as that flowing from the condenser. It could be calculated as,

$$\dot{m}_{12-liq} = \dot{m}_8 (1 - X_8) \tag{5.15}$$

At state 12-liquid, the liquid solution is considered as pure water since all ammonia is already evaporated. Therefore, the obtained refrigerating capacity calculated from equation (5.14) can be considered as the maximum.

After absorption process, the strong solution (10) becomes weak solution (11). Concentration difference between the weak solution and the strong solution was considered as a result of absorption process in the absorber. Concentration of the weak solution is calculated from,

$$X_{11} = \frac{\dot{m}_{10} X_{10} + \dot{m}_{8} X_{8}}{\dot{m}_{10} + \dot{m}_{8} X_{8}}$$
 (5.16),

where $\dot{m}_9 = \dot{m}_{10}$ and $X_9 = X_{10}$.

Mass of solution after absorption process (11) is the summation of the strong solution mass and the mass of evaporated ammonia.

$$\dot{m}_{11} = \dot{m}_{10} + \dot{m}_8 X_8 \tag{5.17}$$

In the evaporator of a DAR, evaporation of ammonia occurs in the atmosphere of an auxiliary gas. The process is similar to the evaporation of water in a tray exposed to the open-air. The evaporation rate is not dependent only on the ammonia mass flow rate. It requires surface area for the evaporation process as well. The evaporated ammonia vapor causes increments in partial pressure of ammonia in the evaporator, which causes increments in evaporation temperature. To maintain the low evaporation temperature, all evaporated ammonia vapor must be absorbed by the strong solution in the absorber.

5.5 Combined evaporator-absorber effectiveness

With greater heat input, pumping effect should be increased as the relationship of the bubble pump as shown in the experimental correlation. Then, the solution circulation rate should be increased. However, absorption capability of the DAR might be restricted due to performance limitation of the evaporator and the absorber. Therefore, absorbability of the strong solution had to be included into the calculation.

The strong solution entering the absorber can absorb evaporated ammonia only once in a circulation cycle. The ammonia vapor is absorbed while the strong solution flowing downward as falling film over the absorption surface area. No matter what the concentration of the weak solution is, absorption process will stop when the solution reaches the bottom of the absorber (13). Moreover, if the period of solution flow on the absorption surface area was short i.e. fast flow, it might not enough to have time for the strong solution to absorb all of the evaporated ammonia. Then, ammonia vapor will be left in the evaporator causing partial pressure of ammonia to increase. Then, the refrigeration temperature is raised resulting in less refrigerating effect due to small temperature difference of evaporated ammonia and chilled water in the evaporator.

An index named a combined evaporator-absorber effectiveness (ϵ) was introduced. Normally, the effectiveness is defined as a ratio of the actual concentration difference to that of the maximum available. The maximum concentration is normally referred as that when weak solution is in equilibrium with temperature and partial pressure in the absorber. However, in this study, the weak solution is not saturated after finishing the absorption process. Then, the combined evaporator-absorber effectiveness definition is altered as the ratio of evaporated ammonia mass rate to the total ammonia available from the condenser.

$$\varepsilon = \frac{\dot{m}_{11} X_{11} - \dot{m}_{10} X_{10}}{\dot{m}_{8} X_{8}} \tag{5.18}$$

Mass of evaporated ammonia is calculated as,

$$\dot{\mathbf{m}}_{12-\mathsf{vap}} = \dot{\mathbf{m}}_{11} \mathbf{X}_{11} - \dot{\mathbf{m}}_{10} \mathbf{X}_{10} \tag{5.19}$$

The refrigerating capacity when including effectiveness into consideration can be determined as,

$$\dot{Q}_{evap} = \dot{m}_{12-vap} (h_{12-vap} - h_8)$$
 (5.20)

Liquid refrigerant left at bottom of the evaporator flows back to bottom of the absorber having mass flow rate and concentration of,

$$\dot{m}_{12-liq} = \dot{m}_8 - \dot{m}_{12-vap} \tag{5.21}$$

$$X_{12-liq} = \frac{\dot{m}_8 X_8 - (\dot{m}_{11} X_{11} - \dot{m}_{10} X_{10})}{\dot{m}_{12-liq}}$$
(5.22)

The calculated results must be verified by employing mass balance of both ammonia and water in the solution as,

$$X_{13} = \frac{\dot{m}_{11}X_{11} + \dot{m}_{12-liq}X_{12-liq}}{\dot{m}_{11} + \dot{m}_{12-liq}}$$
(5.23)

This figure, X_{13} , must correspond to the concentration of compressed liquid solution entering the generator (X_1) . Heat released due to absorption process from the absorber could be calculated from

$$\dot{Q}_{abs} = \dot{m}_{10}h_{10} + \dot{m}_{12-vap}h_{12-vap} + \dot{m}_{12-liq}h_{12-liq} - \dot{m}_{13}h_{13}$$
 (5.24)

In the absorber, the absorption rate depends on the solution mass flow rate, concentration of strong solution, surface area of absorption, period of absorption etc. Mass flow rate of the strong solution is affected by the bubble pump performance. Thus, various factors are found to affect the evaporation rate in the evaporator. It seems to be that ammonia cannot completely evaporate in the evaporator. The liquid ammonia that is not evaporated will return to the absorber without producing any cooling effect.

5.6 Solution heat exchanger (SHX)

The weak solution flowing out from the absorber into the solution heat exchanger, SHX, will be preheated. It is assumed that there is no heat loss to the surroundings from the SHX. Therefore, the amount of heat transfer internally of the SHX could be balanced as,

$$\dot{m}_{13}(h_1 - h_{13}) = \dot{m}_9(h_9 - h_{10})$$
 (5.25)

5.7 Coefficient of Performance

Since DAR is a refrigeration system that uses only heat as input power to drive the system, the coefficient of performance (COP) of the DAR is defined as,

$$COP = \frac{\dot{Q}_{evap}}{\dot{Q}_{in}}$$
 (5.26)

5.8 Conclusion

A mathematical model was developed to analyze thermodynamic performance of the experimental DAR. The model was developed in order to be used for calculation of the maximum performance under given operating conditions. When calculated results are compared with actual values obtained from the experimental refrigerator, it will show that how losses at different devices occurred and how the system can be modified to improve its performance.

CHAPTER VI

Test Results and Discussion

This chapter provides the experimental and calculation results obtained from the experimental DAR. The effects of heat input to the generator, rectifier temperature, and auxiliary gas pressure on the system performance are presented. During the tests, while one parameter was varied the other two were maintained. It was tested with the generator heat input between 1000 to 2500 W, helium pressure of 6.0 to 10 bar. The rectification temperature was set between 50 and 90°C.

Cooling capacity between 100 to 200 W and COP between 0.07 to 0.17 was obtained. The actual results are compared with calculated values based on the model developed in chapter 5. Actual performances were found to depend on the evaporator and absorber mass transfer performance. The bubble pump characteristic was also found to be an important parameter.

6.1 Experimental procedure

During the tests, performance parameters such as temperatures, pressures, heat input to the generator, and cooling capacity were recorded. The heat input to the generator was equal to the electrical power supplied to the heater. Cooling load to the evaporator was provided by mean of circulation of water through the evaporator coil. For each test, 30 kg of fresh water in a well-insulated icebox was chilled from 30°C down to 0°C. A small aquarium pump (17 W) was used to circulate the water. During the tests, it was found that temperature of the chilled water decreased at an almost constant rate. Thus it might be considered that the cooling capacity was independent from the water temperature

or constant throughout the operating period. Therefore, the cooling capacity at the evaporator could be determined as:

$$\dot{Q}_{\text{evap}} = \frac{m_{\text{water}} Cp(T_2 - T_1)}{\Delta t} + 17 \text{ W}$$
(6.1)

where m_{water} mass of water in the icebox (30 kg)

C_p specific heat capacity of water (4200 J·kg⁻¹·K⁻¹)

 T_1 the starting temperature (30°C)

 T_2 the final temperature (0°C)

 Δt time (second)

Coefficient of Performance was then obtained from:

$$COP = \frac{\dot{Q}_{evaporator}}{\dot{Q}_{generator}}$$
 (6.2)

COP obtained from the above equation was a measure of overall performance and included all the unwanted heat losses and gains to the system.

Before the tests, the system was evacuated. The absorber and generator were filled with 7 liters aqueous solution of ammonia with mass concentration of 0.25. The system was left to reach equilibrium with surrounding. Then it was charged with helium until the required pressure was achieved.

6.2 Effect of the generator heat input to the system performance

Figures 6.1 and 6.2 show plots of cooling capacity and COP of the experimental refrigerator. It was operated over a range of generator heat input. It was charged with helium pressure of 6.8 bar and operated within rectification temperature range of 75-80°C. It was discovered that there was a minimum generator heat input required to start the experimental refrigerator. Below the minimum heat input, it would not operate or produce any cooling effect. When the heat input was increased beyond the minimum value, the obtained cooling capacity increased sharply. As the heat input was increased further, the

cooling capacity increased slightly. Variation of the COP was similar to the cooling capacity when the heat input was low. However, the COP increased to a maximum value, then it dropped as the heat input continued to increase. It contrasted with the case of the cooling capacity, which continued to increase.

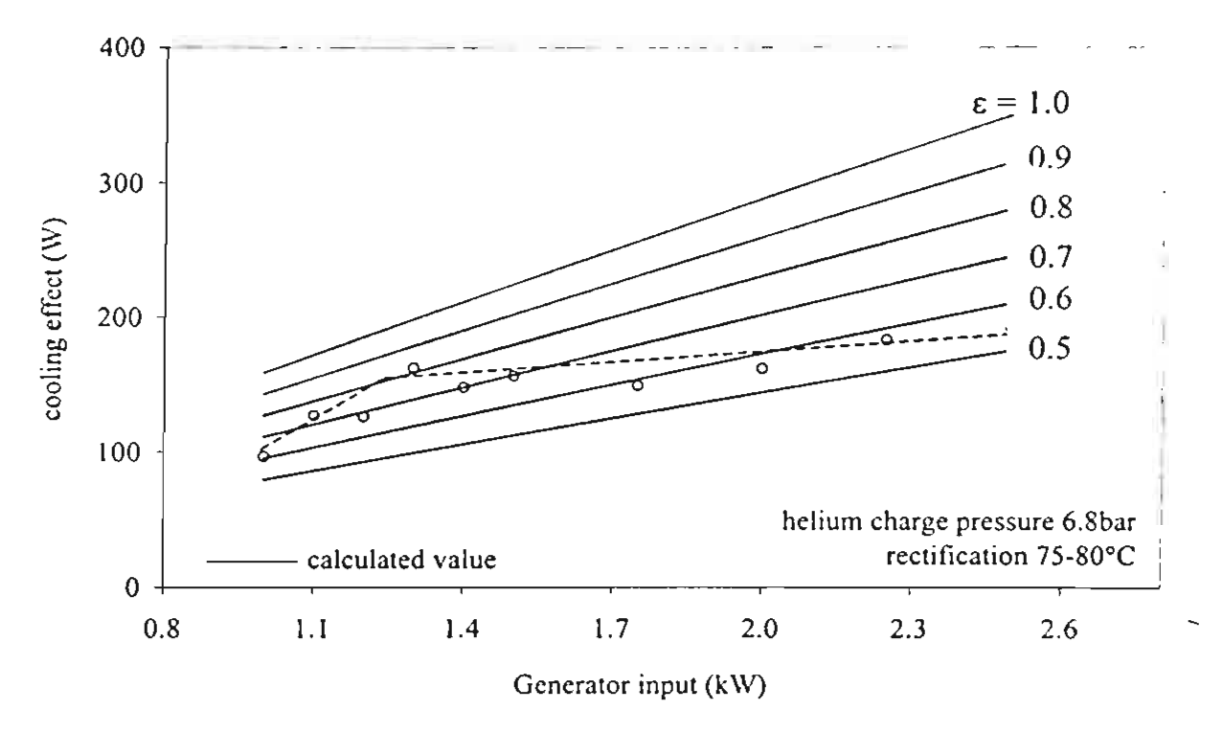


Figure 6.1 Cooling effect of the system with variation of input heat at the generator.

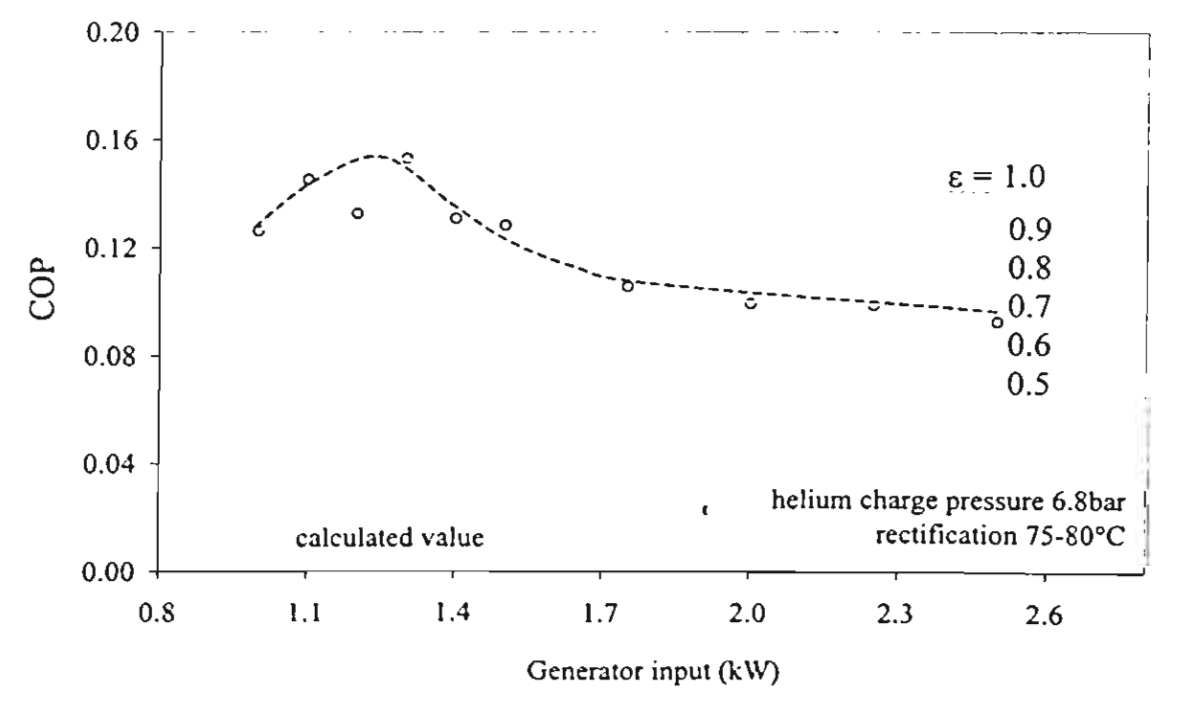


Figure 6.2 COP of the system with variation of input heat.

When the generator heat input is lower than the minimum value, the system cannot produce any cooling effect. This is due to the bubble pump characteristics. To obtain a pumping effect, a minimum vapor generated is required. When the heat input is too low, there is not enough vapor to drive the pump. This means that only the refrigerant vapor is produced. This refrigerant will be liquefied and enter the evaporator. However, it cannot evaporate and produce any cooling effect since there is no liquid flowing to induce absorption of the refrigerant vapor. When the heat input is increased beyond the minimum value, the pumping effect occurs. The liquid will be circulated to the absorber and absorb the refrigerant vapor. Thus, a cooling effect is produced. Further increase in heat input will produce a higher cooling effect as more refrigerant vapor is generated and more liquid is pumped to the absorber. This also causes the COP to increase. From figure 6.1, it can be seen that when the heat input continues to increase beyond a certain point (about 1300 W), the cooling capacity will increase with a lower rate. This implies that the cooling capacity is limited by the evaporator or absorber mass transfer performance. As the increased rate of cooling capacity does not match with the rate of heat input, this results in a drop of the COP.

Cooling capacity is strongly dependent upon the evaporation and absorption rates, which depend on area of wetted surface. To evaporate all refrigerant, there must be enough surface for evaporation (the evaporator coil on which the liquid refrigerant is evaporated) and enough surface for absorption (absorber column on which the ammonia vapor is absorbed). When there is an increase in the generator heat input the mass flow of ammonia is increased. However, the evaporator and absorber surfaces are fixed. This may not be enough for all the ammonia to evaporate or to be absorbed. When the refrigerant flow is increased due to the increased generator heat input, the cooling capacity might not increase. This is because it cannot be completely evaporated or absorbed. It should be

noted that during the tests, it was observed through the sight glass that the absorber column and evaporator coil were not completely covered with liquid.

When the liquid refrigerant is completely evaporated in the evaporator, the concentration of solution obtained at the end of the absorber column is equal to that accumulated at the bottom of the absorber. If the ammonia cannot completely evaporate, the concentration of solution obtained at the end of the absorber column is lower than that accumulated at the bottom of the absorber. For the first case, the absorber-evaporator effectiveness (equation 5.18) is exactly equal to unity. For the second case, the effectiveness is lower than one.

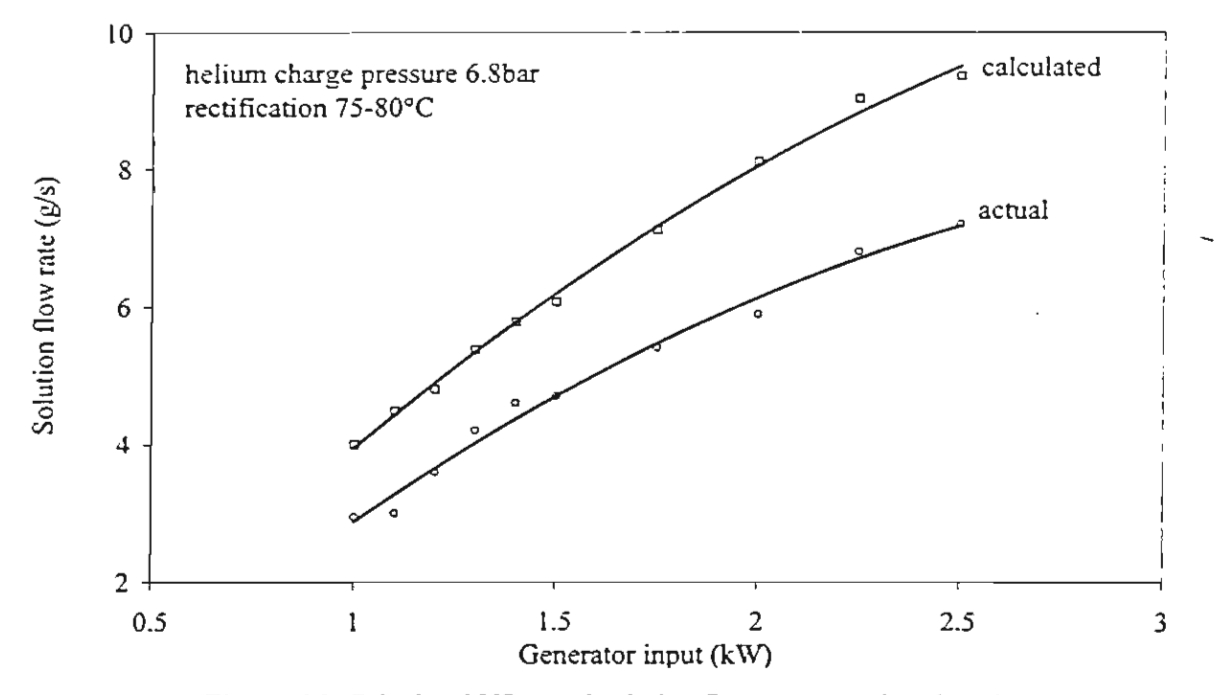


Figure 6.3 Calculated VS actual solution flow rate at various heat input.

Comparisons of actual and calculated mass flow rate of liquid solution through the pump tube versus generator input are provided in Figure 6.3. The actual results were found to lie between 70 to 80% of the calculated values. The difference may result from heat loss from the generator and pump tube. At the generator, it causes less vapor to be generated. At the pump tube, it causes condensation of the vapor. Other reasons may be the properties of the fluid. The pump performance (equation 5.3) was obtained using air

and water as the test fluid rather than aqueous ammonia solution. It must be noted that if 10% heat loss is included, the calculated values will be closer to the actual values.

Referring to the figures 6.1 and 6.2, it can be seen that the calculated cooling capacity increases almost linearly with the generator heat input. When there is an increase in the generator input, more vapor is generated and more liquid is pumped. This causes more refrigerant to enter the evaporator and more liquid to enter the absorber. Based on the model developed with an effectiveness of one, all liquid refrigerant is evaporated in the evaporator and maximum cooling capacity is obtained. When the effectiveness is reduced, all liquid refrigerant does not completely evaporate in the evaporator. The cooling capacity drops and the unevaporated liquid just returns to the absorber without producing any cooling effect.

At a heat input approximately below 1300 W, both actual and calculated cooling capacity increase with the generator heat input. It can be noted that the actual cooling capacity is compatible with calculated value with effectiveness between 0.5 and 0.7. It could be implied to be a result of the absorber and evaporator performance. To absorb refrigerant vapor into solution or to evaporate liquid refrigerant, a certain amount of wetted surface area is required. With low heat input, the amount of liquid refrigerant entering the evaporator and liquid solution entering the absorber is small. Liquid film cannot be formed properly on the evaporator coil as well as on the absorber column. This reduces the evaporation and absorption rates, which effects the cooling capacity. Thus the actual cooling capacity is compatible with the calculated value of low effectiveness. As the heat input increases, more refrigerant and solution are circulated in the system, and a better liquid film on the absorber column and on the evaporator coil will be obtained, this results in better evaporation and absorption rates. Therefore, the actual cooling capacity is compatible with calculated values having high effectiveness.

For the generator input greater than 1300 W, the actual cooling capacity was almost constant (slightly increasing with heat input). Even though more refrigerant is generated with increased heat input, the cooling capacity is fairly constant due to limited mass transfer surfaces of the evaporator and the absorber. The slight increment may result from higher mass transfer coefficient due to an increase of solution flow rate. This resulted in a drop of effectiveness when compared with the calculated value.

6.3 Effect of helium charged pressure on the system performance

Helium charge pressure is a key parameter in the operation of the DAR. The system will fail to operate if the charge is too low. However, overcharge of helium will cause too high operating pressure due to existence of partial pressure of ammonia in the condenser. This can be realized by comparing the actual system pressure and ammonia saturation pressure at the condenser temperature.

The bubble pump can be driven by vaporized solution in the generator. According to the actual results and mathematical model discussed in chapters 4 and 5, performance of the bubble pump depends on the amount of vapor volume. The higher the generator heat input, the more vapor is generated. Knowing that specific volume of any vapor varies with its pressure, for the same mass of vapor generated, its volume should be less when the system pressure is increased. Therefore, the helium charge pressure should affect performance of the bubble pump. For a given heat input to the generator, when the helium charge pressure is increased, the amount of liquid being pumped is decreased.

The experimental refrigerator was charged with helium pressure of 6.1, 6.8, and 10.2 bar. These pressures were measured when the system was not operated. It was found that helium charge pressure caused effect on system performance, cooling capacity, COP, and minimum generator heat input requirement.

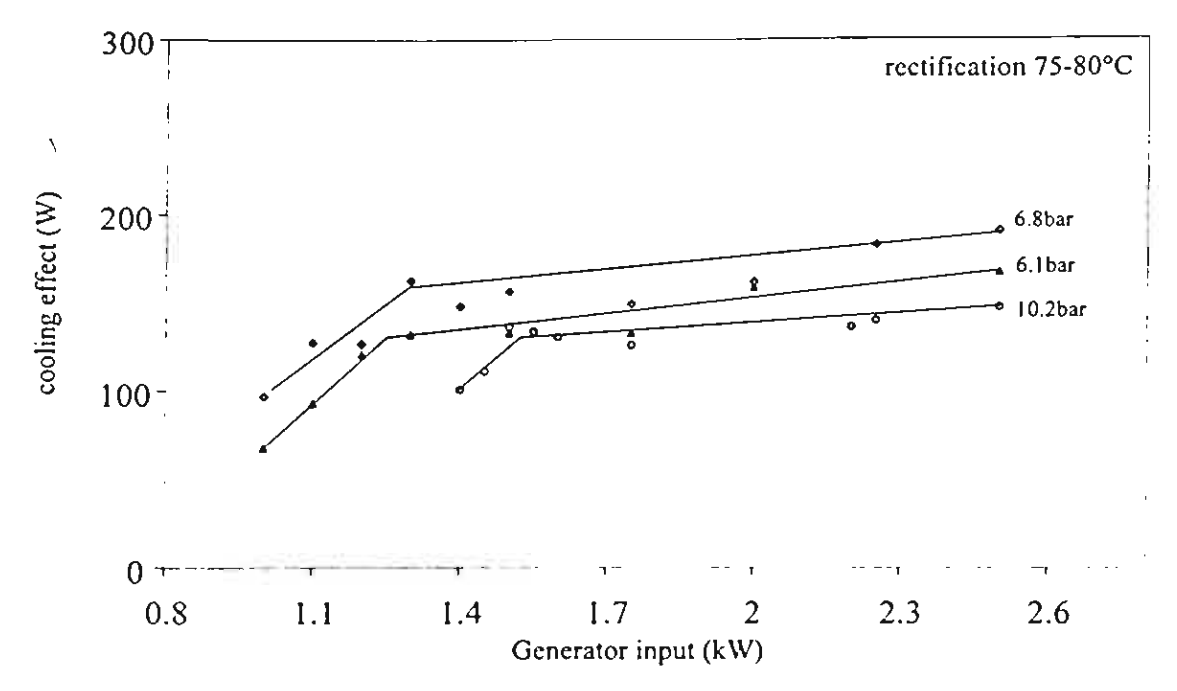


Figure 6.4 Cooling capacity with variation of heat input at various helium charge pressure.

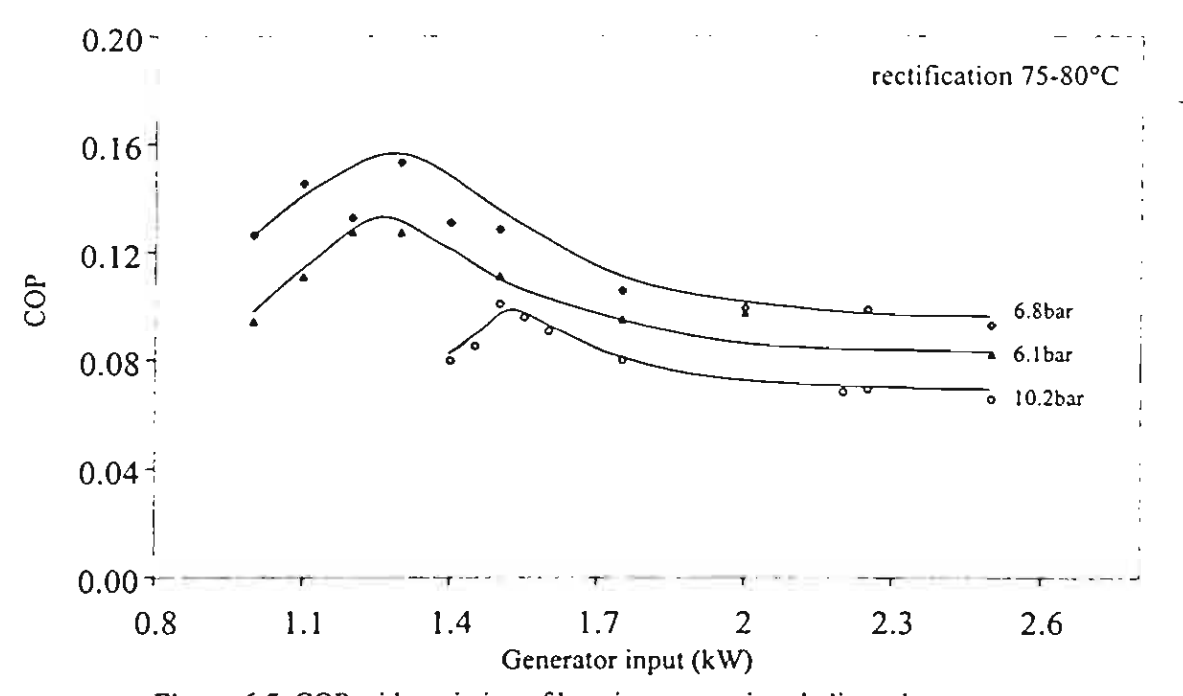


Figure 6.5 COP with variation of heat input at various helium charge pressure.

The minimum heat input required was shifted to the higher value when the helium charge pressure was increased from 6.8 to 10.2 bars as shown in Figure 6.4. For the same amount of heat input to the generator, the amount of refrigerant generated was slightly increased (as less liquid was pumped and more heat was used to generate the vapor) when

the helium charged pressure increased. However, the cooling capacity dropped with increased helium charge pressure. It would result from less liquid solution circulating in the absorber. Thus less ammonia could be absorbed and so a reduction of cooling effect was obtained.

When the helium charge pressure was increased from 6.1 to 6.8 bar, the effect of helium charge pressure to the minimum heat input required was not significant. It is not clearly shown on the figures. However, it can be expected that the effect of helium charge pressure to the bubble-pump performance would be similar to that for the previous case. In contrast with the previous case, it was found that the cooling capacity and COP dropped with decrement of helium charge pressure from 6.8 to 6.1bar. The drop of cooling capacity (even more liquid solution is pumped and circulated in the absorber) could result from increment of ammonia evaporation temperature in the evaporator. With decreased helium charge pressure, the ammonia partial pressure in the evaporator will increase. It causes a higher ammonia evaporation (saturation) temperature. As the differential temperature between ammonia (evaporate outside the coil) and chilled water (circulate in the coil) is reduced, the heat transfer rate will drop. This causes less ammonia to evaporate and certainly less cooling effect is produced.

Too much helium charged will reduce the liquid solution entering the absorber. It reduces the absorption capability and cooling capacity. Too low helium charge pressure, the ammonia partial pressure in the evaporator is high. This results in the ammonia evaporating at high temperature in the evaporator. As the differential temperature between refrigerant and chilled water reduce, less heat transfer capability to the ammonia and less cooling capacity would exist. It may be implied that for each operating condition, there is an optimum helium charge pressure.

6.4 Effect of rectification temperature on the system performance

The major disadvantage of using ammonia/water as working fluid is that at the generator water always evaporates with ammonia. Without a rectifier, the contaminated ammonia vapor will be liquefied and passed into the evaporator. In the evaporator, water causes ammonia to evaporate at a higher temperature for a given pressure. Thus, the unwanted evaporated water vapor will degrade the system performance. To enhance the system performance, a rectifier is needed to purify ammonia vapor before being liquefied in the condenser.

Figure 6.6 shows rectification process on a P-T-X-h diagram. The ammonia vapor leaving the separator (4) contains some water. The vapor is purified by being cooled in the rectifier (6). It condenses some ammonia and some water vapor as condensate (5). Therefore, the concentration and purity of vapor ammonia exiting the rectifier is increased (7). Relations between the mass entering and exiting the rectifier are:

$$\frac{\dot{m}_5}{\dot{m}_6} = \frac{X_7 - X_6}{X_7 - X_5} = \frac{h_7 - h_6}{h_7 - h_5}$$
(6.3)

$$\frac{\dot{m}_7}{\dot{m}_6} = \frac{X_6 - X_5}{X_7 - X_5} = \frac{h_6 - h_5}{h_7 - h_5}$$
(6.4)

These mass ratios can be obtained graphically as,

$$\frac{\dot{m}_5}{\dot{m}_6} = \frac{\overline{67}}{\overline{57}} \tag{6.5}$$

$$\frac{\dot{m}_7}{\dot{m}_6} = \frac{56}{57} \tag{6.6}$$

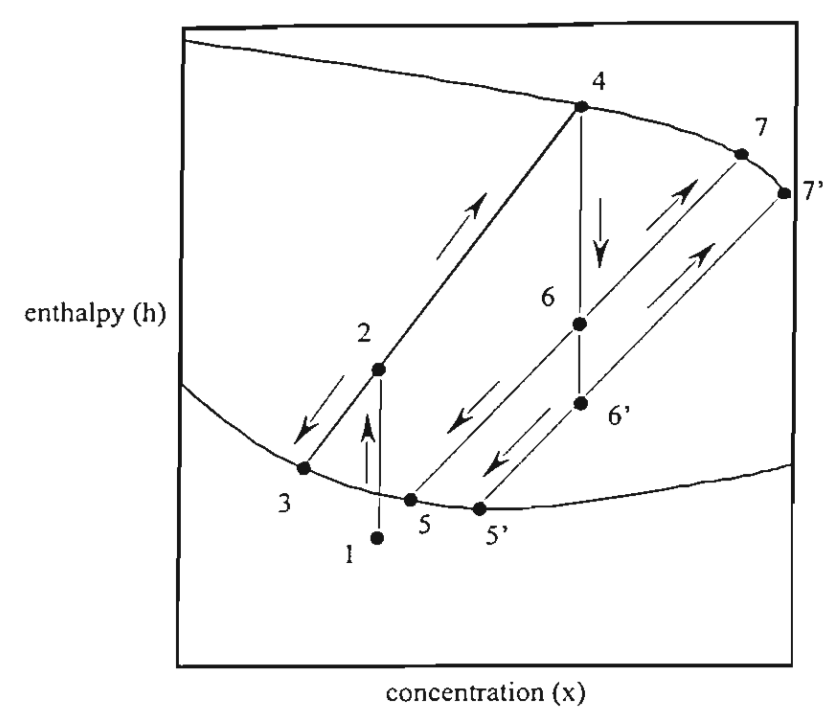


Figure 6.6 Generator and separator's process on P-T-X-h diagram.

Referring to Figure 6.6, if the rectification temperature is reduced from 6 to 6', the vapor will leave the rectifier at a higher concentration (7') but at a lower quantity. The variation of rectification temperature effects the system performance. A higher rectification temperature yields more ammonia vapor having lower purity, while a lower rectification temperature gives less amount of ammonia but having higher purity.

Figures 6.7 and 6.8 show effects of rectification temperature on the system performance. They also show the calculated results compared with the actual values. From these Figures, it can be seen that the calculated cooling capacity and COP increase with the rectification temperature. This implies that, at a higher rectification temperature, more ammonia enters the evaporator and produces a higher cooling effect than at a lower rectification temperature. However, from the tests, the cooling capacity was fairly constant. The constant of the cooling capacity may result from low mass transfer performance of the absorber and the evaporator.

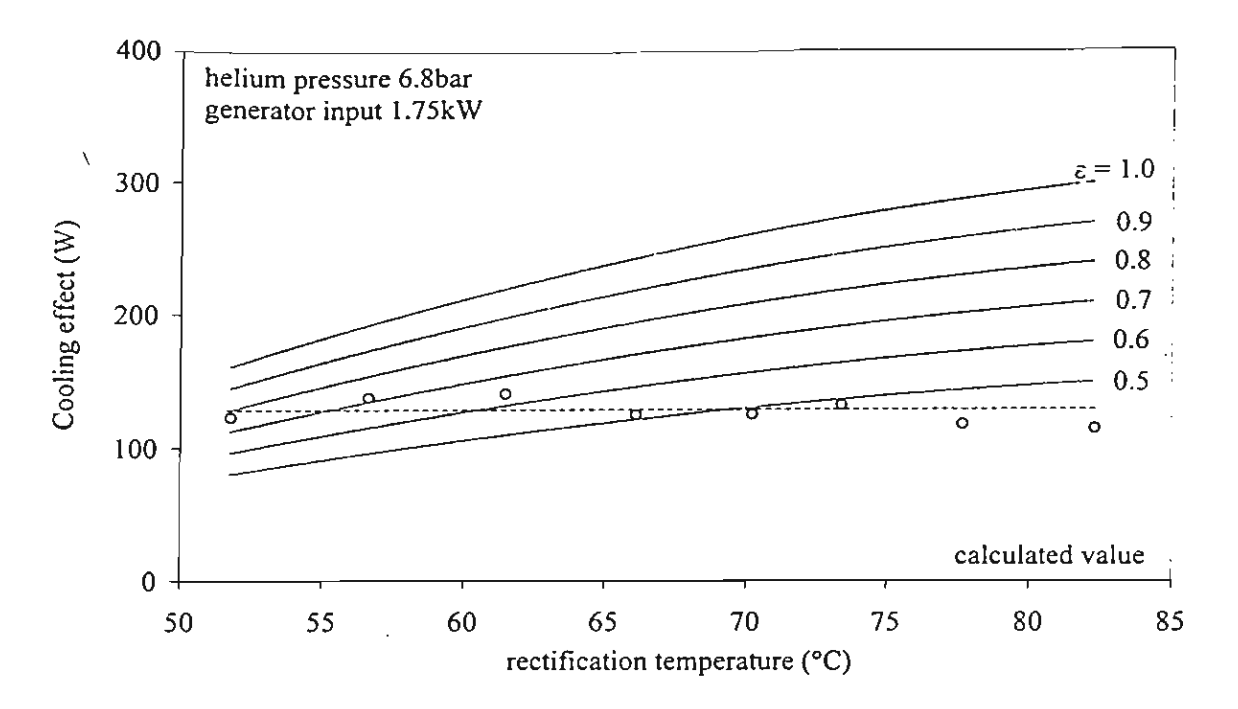


Figure 6.7 Comparison of experimental and calculated cooling capacity with variation of rectification temperature.

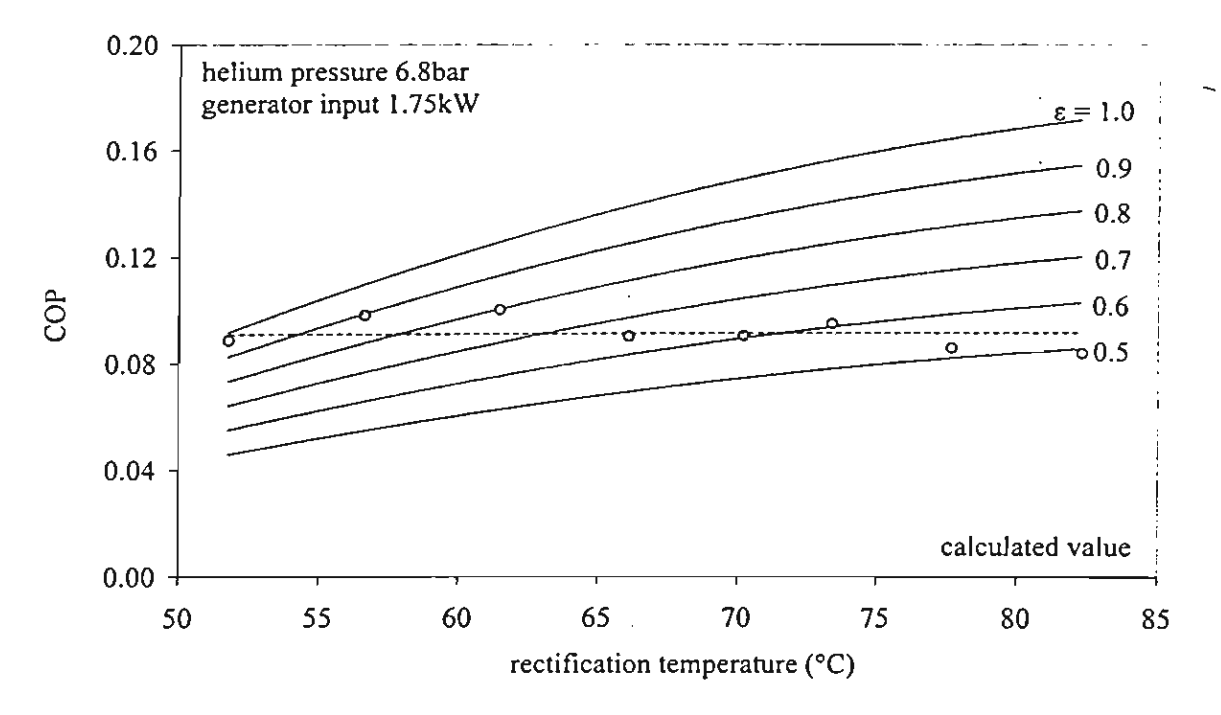


Figure 6.8 Comparison of experimental and calculated COP with variation of rectification temperature.

Alternatively, at a high rectification temperature, the purity of ammonia is low thus it evaporates at relatively high temperature in the evaporator. This results in a low differential temperature between the ammonia and the chilled water. Therefore, the cooling

capacity remained unchanged even though there was more ammonia entering the evaporator.

6.5 Conclusion

The tested DAR was clearly found to be affected by variation of heat input at the generator and auxiliary gas charge pressure. There were related to each other. There was a minimum heat input level required to start the system operation. At a lower heat input than the minimum value, the system could not be operated. Increment of heat input increased the cooling effect until a transition point (maximum COP) was reached. Increased heat input beyond this point would not increase the cooling effect much. Thus, the COP was reduced with greater heat input beyond the transition point.

The minimum heat input required to start the system operation is affected by the auxiliary gas charge pressure. The required heat input level to start the system was greater with higher auxiliary gas charge pressure. It could occur as a result of less specific volume of vaporized solution in more pressurized system for a given mass of solution. Therefore, the onset of the bubble pump operation was shifted to a higher heat input level. However, with low helium charge pressure, the system was found to operate with lower performance. It could result from high partial pressure of ammonia in the evaporator, which increased the evaporation temperature of ammonia. Heat transfer performance should be reduced due to less temperature different between evaporated ammonia and chilled water circulated through the evaporator coil.

There was no significant effect obtained from the experimental results with variation of the rectification temperature. It was found that variation of the rectification temperature did not cause any effect on the bubble pump. The increased rectification temperature gave more refrigerant at the condenser but with less purity. It did not cause

any increment of the absorption capability as the pumped solution was consistent. Therefore, there was no effect to the cooling capacity due to increased rectification temperature. Reduction of the rectification temperature did not affect the actual cooling capacity either.

CHAPTER VII

Recommendations for System Improvement

According to the experimental results described in chapter 6, performance of DAR was relatively poor compared with other refrigeration systems. In the past, many researchers tried to improve its performance as discussed in chapter 2. Heat recovery within the system was an option proposed in the literature. In the DAR, heat input is supplied only at the generator while the other components reject or lose heat to the surroundings.

To improve the system performance, heat transferred in all components should be calculated so that the analysis could be more precise. Any modification carried out to improve the system performance can be done pertinently. Based on the mathematical model proposed in chapter 5, some calculation samples are presented in this chapter. The calculation model can be used as an effective tool for determination of the system heat balance. An experimental result was used as a calculation example. The operating conditions are tabulated in Table 7.1.

Table 7.1 An operating condition used for heat balance calculation

operating pressure	13.3bar
cooling water temperature	30-32°C.
rectification temperature (averaged)	75-80°C
auxiliary gas charge (initially)	6.1bar
solution concentration	0.23
mass of chilled water	30kg.
chill water temperature	30 down to 0°C.
heat input at the generator	1.3kW.

7.1 Increase evaporator and absorber mass transfer performance

According to the discussion provided in chapter 6, it was found that after the system was operated continuously, cooling capacity of the system was limited. Increment of system heat input did not raise much of the cooling effect when the system limit was reached. It was proposed that this limitation occurred as a result of limitation in the absorption and evaporation capabilities. It could be occurred by too little absorption or evaporation from wetted areas. Or it could occur from too short a period due to fast flow of the fluid. To improve the system performance, these two factors must be considered simultaneously.

Table 7.2 Comparison of modified systems

	energy transfer (W)					energy transfer (%)				
	A	В.	Ç	D.	E	A	В	C	D	E
generator heat input	1322*	1322	2992	962	966	100.0	100.0	100.0	100.0	100.0
evaporator heat input	135°	174	174	174	174	10.2	13.2	5:8	18.0	18.0
total energy input	1457*	1496	3166	1136	1140	110.2	113.2	105.8	118.0	118.0
								•		
absorber heat reject	899	936	2606	576	936	68.0	70.8	87.1	59.9	96.9
condenser heat reject	202	202	202	202	202	15.3	15.3	6.7	21.0	20.9
rectifier heat reject	356	356	356	356	0	26.9	26.9	11.9	37.0	0
total heat reject	1457	1494	3164	1134	1138	110.2	113.0	105.7	117.9	117.8
heat transfer at solution										
heat exchanger	1505	1670	0	2030	1670	113.8	126.3	0	211.0	172.9

obtained from the experiment

The evap.-abs. ε is defined by equation 5-18.

The SHX
$$\epsilon$$
 is defined as $\frac{t_9 - t_{10}}{t_9 - t_{13}}$.

Table 7.2 shows calculated results based on experimental conditions listed in table 7.1. The sum of heat input at the generator and at the evaporator is equal to the sum of heat rejected at the absorber, the condenser, and the rectifier. Percentage value of the

A: based on the experiment (estimated evap.-abs. $\varepsilon = 0.8$, and estimated SHX $\varepsilon = 0.7$)

B: with evap.-abs. $\varepsilon = 1.0$

C: without the SHX (evap.-abs. $\varepsilon = 1.0$, and SHX $\varepsilon = 0$)

D: increased SHX effectiveness (evap.-abs. $\varepsilon = 1.0$, SHX $\varepsilon = 0.9$)

E: heat recovery from the rectifier (evap.-abs. $\varepsilon = 1.0$, and SHX $\varepsilon = 0.7$)

evaporator input, which is a ratio of the heat input at the evaporator to that at the generator, is recognized as the COP of the system. Based on the experimental refrigerator, column A, the heat input to the evaporator or cooling capacity is 135W or 10.2% of the generator input. When compared with the calculated value, the absorber-evaporator effectiveness is estimated to be around 0.8.

The low effectiveness value results from imperfect evaporation or absorption processes. If a better evaporator and absorber are used, a higher cooling capacity will be achieved. If the ammonia is completely evaporated and absorbed, the evaporator and absorber effectiveness is unity as listed in column B. It should be noted that the COP and cooling capacity can be increased by up to 29% by improving the evaporator and absorber performances as shown in column B.

7.2 Increase the solution heat exchanger effectiveness

According to the performance of the experimental refrigerator, column A, it can be noted that recovered heat at the solution heat exchanger is surprisingly high. The heat exchanger recovered 1505 W of heat, which is 1.14 times of the generator input. This high heat recovery value can be confirmed by the time required for the start up period. After transferring heat to the generator, it took almost an hour before the cooling effect could be produced. The heat input to the generator was accumulated in the working fluid and recovered internally at the solution heat exchanger.

If the solution heat exchanger is excluded from the experimental refrigerator, the system performance will drop drastically. Heat input must be increased to compensate the disappeared amount of heat from the solution heat exchanger. Heat balance of the system excluding the heat exchanger is shown in column C. It is found that heat input increased up to 3kW and the COP dropped drastically to 0.06. At the same time, heat rejected at the

absorber is increased. The strong solution flowing from the separator is hot. Its temperature is a little bit lower than temperature of the pumped liquid. Therefore, the absorption capability might drop due to this high temperature of the strong solution entering the absorber. Therefore, the obtained cooling capacity might be lower than the proposed result, depending on the absorption capability of the strong solution.

Based on the experimental results, the solution heat exchanger effectiveness is estimated to be around 0.7. If a larger heat exchanger with effectiveness of 0.9 is used, the heat recovered will be increased to 2030W. This results in a higher solution temperature at the generator and a cooler solution temperature at the absorber inlet. The heat input at the generator and heat rejected at the absorber will reduce to 962W and 576W respectively as shown in column D. It results in the COP increasing up to 0.18, which is 76% improvement over the experimental refrigerator or 210% improvement over the system without a solution heat exchanger.

7.3 Recover heat from the rectifier

According to table 7.3, at the rectifier (location 5, 6, and 7), the operating temperature is reduced as a result of rectification process. It is reduced from the generator temperature, 141.3°C, down to the rectification temperature, 73.2°C. Heat is rejected from the rectified refrigerant vapor so as to partially condense the solution. From the calculated result of heat balance shown in table 7.2, the rejected heat from the rectifier is 356W. This amount of heat is released to the cooling water supply at the rectifier. Since the temperature of this amount of heat is high, the waste heat can be recovered for transferring to solution as input heat.

It was found that this amount of rejected heat could be used to improve the system performance. It can be transferred to the generator as its temperature is high enough. If all

the rectification heat is transferred to the generator rather than reject to the ambient, the generator input will reduce by the same amount as the heat rejected at the rectifier. The calculated results, column E, show that percentage of heat saving at the generator is 27% of input heat of case B. This results in an improvement of system COP up to 38%.

Table 7.3 Properties of working solution in column B

 $\varepsilon = 1.0$

location	T (°C)	X	h (kJ/kg)	m (g/se	c) phase
1	112.0	0.225	328.7	5.538	liquid
2	141.3	0.225	567.4	5.538	mixture
3	141.3	0.192	476.3	5.216	sat liquid
4	141.3	0.750	1851.7	0.322	sat vapor
5	73.2	0.517	84.3	0.162	sat liquid
6	73.2	0.750	717.6	0.322	mixture
7	73.2	0.985	1418.1	0.160	sat vapor
8	36.0	0.985	156.0	0.160	liquid
9	139.6	0.202	462.1	5.377	liquid
10	70.8	0.202	151.5	5.377	liquid
11	45.8	0.225	27.1	5.535	liquid
12 liq	0.0	0.000	-0.04	0.002	liquid
12 vap	0.0	1.000	1264.9	0.158	vapor
13	45.8	0.225	27.1	5.538	liquid
					•

7.4 Redesign of the bubble pump

According to the discussion in chapter 6, the DAR operation was not consistent. It had an optimum operating range, which differed from one operating condition to another. The bubble pump operation dominated the operating condition. The DAR cannot be operated unless the bubble pump is started. After the system is started, the bubble pump still dominates the system operating characteristics. The bubble pump operation is dependent upon some parameters such as head ratio, pump tube size, and length, etc.

To improve the system performance, the bubble pump should be designed in a manner so that the vapor generated corresponds to the pumped solution. This should be realized at the beginning of the design stage. The absorption capability is limited by flowing characteristics of the strong solution. Therefore, the bubble pump should be

redesigned in a manner that the generated vapor would correspond to the amount of the pumped liquid solution.

Cooling capacity is not only dependent on the amount of refrigerant flow but it also relies on the liquid solution circulation rate. The system will provide maximum COP when the refrigerant is completely evaporated in the evaporator. This can be achieved only when there is enough solution circulating in the absorber. If there is too much refrigerant for the solution to absorb, the unevaporated refrigerant will return to the absorber in liquid phase without producing any refrigeration effect. This can be considered as waste, since heat is always required to produce the refrigerant vapor. If there is too much solution circulating in the absorber, the refrigerant will be completely evaporated in the evaporator. However, this can be considered as waste, since the cold solution from the absorber is heated at the pumping boiler. Then it is returned to and cooled down in the absorber without absorbing the refrigerant vapor. As the amount of refrigerant and solution flow rate is depended on the bubble pump design, it can be implied that the bubble pump is a critical component in a design of DAR.

7.5 Proper charge of the auxiliary gas

It was shown in chapter 6 that the auxiliary gas charge pressure caused different characteristics in the DAR operation. Too low or too high auxiliary gas charge pressure caused the DAR operating performance to become lower. Too low auxiliary gas charge increased partial pressure of ammonia in the evaporator, resulting in a higher temperature of evaporation. Then, temperature difference of the evaporation and chilled water temperature was reduced. Resulting in lower cooling capacity, the system performance was degraded. However, too high charge pressure of the auxiliary gas, overcharged, also degraded the operating performance of the system. As the system is more pressurized,

specific volume of the vaporized solution based on the same mass basis is decreased. The minimum heat input required to start the system is increased due to increased heat input required to start the bubble pump.

The operating temperature at the generator is elevated with increased operating pressure, which resulted from the auxiliary gas charge pressure. With overcharged auxiliary gas, operating temperature of the systems is raised. Higher operating temperature causes greater heat losses from the system due to greater temperature difference between the system and the ambient, which degraded the system performance.

To optimize the system performance, the auxiliary gas must be properly charged otherwise, the system will be operated inefficiently. However, the auxiliary gas charge pressure cannot be specified exactly. It is dependent upon the system application and surrounding conditions.

7.6 Conclusion

The DAR was analyzed theoretically based on the experimental results. Four alternatives are proposed for implementation with the system to enhance the performance. Heat recovery from the rectifier is shown to reduce heat input at the generator so that the performance can be increased. To implement with the system, the generator, the bubble pump, the separator, and the rectifier must be rearranged so that the rectification heat could be transferred to the generator. Redesign of the bubble pump and the absorber is another option that could be useful. The new-design bubble pump ought to be operated with the proper ratio of pumped liquid solution and vaporized solution. Then, all of the evaporated solution can be absorbed back to the strong solution in the absorber resulting in the better performance. The third choice is to increase the heat exchanger effectiveness of the SHX. It can be easily done by enlarge the SHX. Then, the absorption capability of the strong

solution at the absorber inlet can be increased too. At the same time, the generator heat input could be reduced. Finally, it is recommended that the auxiliary gas charge pressure should be properly considered. As the system operation is directly affected by this parameter. Proper gas charge could help the system to reduce heat loss due to temperature difference of the system and surroundings. It also increased heat transfer capability in the evaporator by maintaining the optimum partial pressure of ammonia in both evaporator and condenser. However, the proper amount of auxiliary gas charge pressure cannot be exactly specified. It is dependent upon the operating conditions and the system applications.

CHAPTER VIII

Conclusions

This thesis describes an investigation of a diffusion absorption refrigeration cycle (DAR) in both theoretical and experimental terms. The experimental refrigerator was designed and constructed. It was tested with various generator heat inputs, helium charge pressures, and rectification temperatures. The system could produce cooling capacity up to 200 W with COP up to 0.2. A simple mathematical model is also described. The calculated results were used to compare with the actual values.

A bubble-pump, used for circulation of working solution in the system, was studied separately. The actual system is operated under high pressure and using ammonia and water as working fluid, the pump was tested at atmospheric pressure using water and air. The study showed that pump performance depended on its dimensions i.e. tube diameter, tube length, and head ratio. A pump tube with similar geometries to that used in the experimental refrigerator was tested. Its performance equation was also obtained. Then, the bubble pump equation and the first law of thermodynamics were used to develop a simple mathematical model, which was used as an analysis tool for the experimental DAR.

Tested results of the experimental DAR showed that there was a minimum heat input required to start the system operation. In fact, it was required for onset of pumping effect of the bubble pump. Cooling capacity and COP were found to increase sharply as the generator heat input was increased. However, at a point, the COP approached a maximum value. Further increase of the generator heat input caused reduction of COP. At this point, the cooling capacity was almost constant. It might be limited by mass transfer performances of either the absorber or the evaporator. The actual results were also compared with calculated values. It was found that the absorber-evaporator effectiveness

reduced while the actual cooling capacity remaining constant. At effectiveness of one, all the liquid ammonia was assumed to evaporate, and a maximum cooling capacity was obtained.

The optimum helium charge pressure was not found. With low helium charge pressure, the bubble pump performance was high. This might result from changes of specific volume of ammonia vapor with system pressure. For a given generator heat input, liquid solution flow rate through the pump tube was increased with reduced helium charge pressure, which should improve the absorption capability. However, it might degrade the heat transfer performance in the evaporator. At low helium charge pressure, the ammonia partial pressure is high. Thus, it will evaporate at relatively high temperature. This causes reduction of the differential temperature between refrigerant and chilled water. Then, the heat transfer rate will be reduced.

There was no significant effect of the experimental performance due to variations of rectification temperature. The calculated results showed that with lower rectification temperature, the refrigerant produced was less but its purity was increased.

Energy balance obtained from the mathematical model was used as an effective tool to analyze the system performance. It will show how the system can be modified. The most critical components are the evaporator and the absorber. They should be designed so that all liquid ammonia can be completely evaporated (in the evaporator) and absorbed (in the absorber). The bubble pump is also a critical part, as it indicates the mass of refrigerant and solution flow. Too much refrigerant or too much solution flow through the pump tube can be considered as waste because it requires energy to produce. Thus, to obtain a maximum performance, the bubble pump must be designed so that the flow of refrigerant is matched with that of liquid solution.

Heat exchanged at the solution heat exchanger (SHX) was shown to be important in designing of the DAR. The results showed that heat recovered at the SHX was higher than the heat input at the generator and the use of SHX could double the COP. Therefore, the capacity of the SHX should be as large as possible. Use of the SHX also reduced the heat rejected at the absorber and its size.

It may be concluded that, to design a DAR with maximum performance, the first priority should be given to the bubble pump. It must be designed so that, the liquid solution and vapor flows are matched. The second attention is paid to the evaporator and the absorber. They must be designed so that, the liquid ammonia is completely evaporated and absorbed. The solution heat exchanger should be designed with maximum effectiveness. Heat recovery at the rectifier is also important as the rejected heat can be used to preheat the solution entering the generator. Helium charged pressure and rectification temperature must be selected to suit the operating condition.

The DAR is a refrigeration system, which can be considered as a user-friendly system. It is easy for use especially in any areas that no electrical is available. Moreover, it requires little maintenance due to its configuration. According to the prior conclusion remarks, it could be improved to perform better operating performance. However, its operating conditions should be considered carefully to match with the atmosphere of site locations. It has potentials to adapt for using as air conditioner or refrigerator, which operated at higher cooling effect temperature than a freezer. It can also be modified to couple with low-grade heat such as industrial waste heat or even the renewable energy such as solar energy.

REFERENCES

ASHRAE, 1997. Fundamental Volume, ASHRAE Handbook.

Chen J., Kim K.J., Herold, K.E., 1996. Performance enhancement of a diffusion absorption refrigerator, Int. J. Refrig.; 19, 3: 208-218.

Eames, I.W. and Aphornratana, S., 1993. Research on heat-operated heat pumps and refrigerators, Journal of the Institute of Energy, 66, 29-39.

Eber, N., 1975. New compact heat exchangers for absorption cooling units, Paper No. B2.46, Proc XIV Int. Cong. Refrig. Washington DC, USA, 886-892.

Gosney, W.B., 1982. Principles of Refrigeration, Cambridge University Press.

Herold, K.E. and Radermacher, L., 1989. Absorption Heat Pumps, Mechanical Engineering, Aug., 68 – 73

Lucas, P., 1967. A boiler for absorption units of the inert gas type having a wide range of input power, Paper No.3.50, Proc XII Int. Cong. Refrig. Madrid, Spain, 1353-1359.

Narayankhedlar K. G. and Maiya M. P., 1985. Investigation of Triple fluid Vapor Absorption Refrigerator, Int. J. Refrig., Vol.8, 335-342.

Patek J. and Klomfar J., 1995. Simple function for fast calculations of selected thermodynamic properties of ammonia-water system, Int. J. Refrig., Vol. 18, No. 4, 228-234.

Pfaff, M., Saravanan, R., Maiya, M.P. and Murthy, S.S., 1998. Studies on bubble pump for a water-lithium bromide vapour absorption refrigerator, Int. J. Refrig., Vol. 21, No. 4, 452-462.

Platen B.C.V. and Munters C.G., 1928. Refrigerator, U.S. Patent No 1,685,764.

Sellerio, U., 1951. Device to speed the circulation of water solutions in household absorption refrigerators, Proc. VIII Int. Cong. Refrig. London, UK, 453-459.

Srikhirin, P., Aphornratana, S. and Chungpaibulpatana, S., 2001. A review of absorption refrigeration technologies, Renewable and Sustainable Energy Reviews, 5, 343-372.

Stierlin, H., 1967. Latest developments in domestic absorption refrigerators and the future outlook, Paper No. 3.43, Proc. XII, Int. Cong. Refrig. Madrid, Spain, 1323-1337.

Steirlin H. and Ferguson J. R., 1990. Diffusion Absorption Heat Pump (DAHP), ASHRAE Trans., Vol.96, Part 1, 3319-3328.

Threlkeld, J.L., 1970. Thermal Environmental Engineering, 2nd edition, Prentice Hall, Inc. Treybal, R.E., 1968. Mass Transfer operations 2 ^{ed.}, McGraw-Hill Book Company, N.Y.. Watts, F.G. and Gulland, C.K., 1958. Triple fluid vapour-absorption refrigerators, J. Refrig., 1, 107-115.

APPENDIX A

Developments of the experimental set-up

Before being assembled as an experimental refrigerator, as used in the study, which was described in chapter 3, several system configurations were constructed and tested. During the modifications, components were redesigned and changed so that it could be operated as required. This appendix describes design and construction process of the experimental DAR. Problems found are also discussed.

1. The first configuration

A schematic diagram of the experimental DAR in the first configuration is shown in figure A.1. This configuration was arranged so that the liquefied refrigerant from the condenser would be accumulated in the trap. Inside the trap, there was an arrangement of piping so as to prevent helium flowing upward from the evaporator into the condenser during operation. The liquid refrigerant could flow into the evaporator so as to be vaporized. There was an electric heater installed in the evaporator. It was used to supply heat as a simulated cooling load. Its power was convenient to be adjusted while being operated via the DAQ system. The amount of heat supplied by the heater could be measured precisely using a power transducer connected to the DAQ system. Evaporation of liquid refrigerant in the evaporator resulted from boiling. Therefore, cooling effect could be quantified accurately.

In the system described above, the experimental DAR had a pipe connecting the evaporator and the absorber. It was located around 100 mm below the top of both the evaporator and the absorber. The connected pipe was located at the high level position to prevent overflowed liquid refrigerant from the evaporator to the absorber during its

operation. The pipe was designed for the auxiliary gas and vaporized ammonia to flow between the evaporator and the absorber. Therefore, the evaporated ammonia could flow from the evaporator to be absorbed by the falling film of the strong solution in the absorber. The auxiliary gas could flow back and forth between the absorber and the evaporator.

During system commissioning, this design configuration failed to operate. No cooling effect was produced at the evaporator. However, some coolness occurred at the trap, which could be sensed by touching. It appeared at the beginning period of operation. It was observed that there was circulation of the solution in the system. It was observed via sight glasses at the absorber. When applying heat to the electric heater at the evaporator, the liquid refrigerant was boiled. Evaporated ammonia caused rising of pressure inside the evaporator and absorber might be greater than that in the condenser. This could be realized from observation that the liquid refrigerant stopped flowing downward from the trap tank. When heating the evaporator was halted for a while, flowing was continued.

The test rig was modified to solve these problems. It must be disassembled. Before charging a new batch of working fluid the system must evacuated. During disassembly of sight glasses, sealing material (o-ring) was found to be damaged. It was found that sealing material had deformed. The sealing material was made up from VITON, which is normally used as it can withstand high temperature application. It was firstly selected for use with system components that must be operated with high temperature such as separator, rectifier. It was found that VITON could not be used in any application using any form of ammonia. It was replaced by EPDM, which was claimed to be compatible with ammonia vapor, liquid ammonia, and aqueous ammonia.

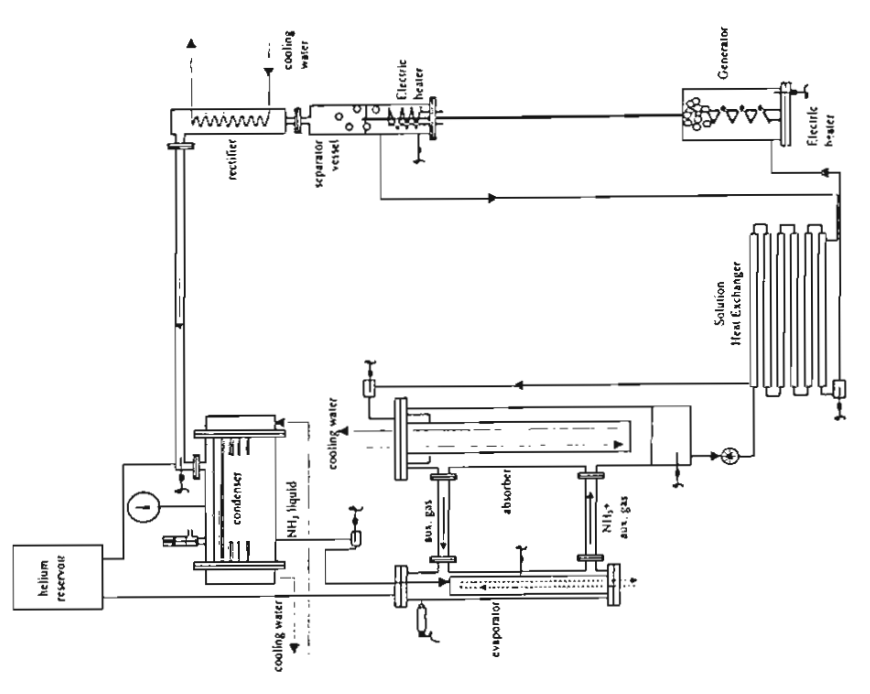




Figure A.1 The first configuration of the experimental DAR.

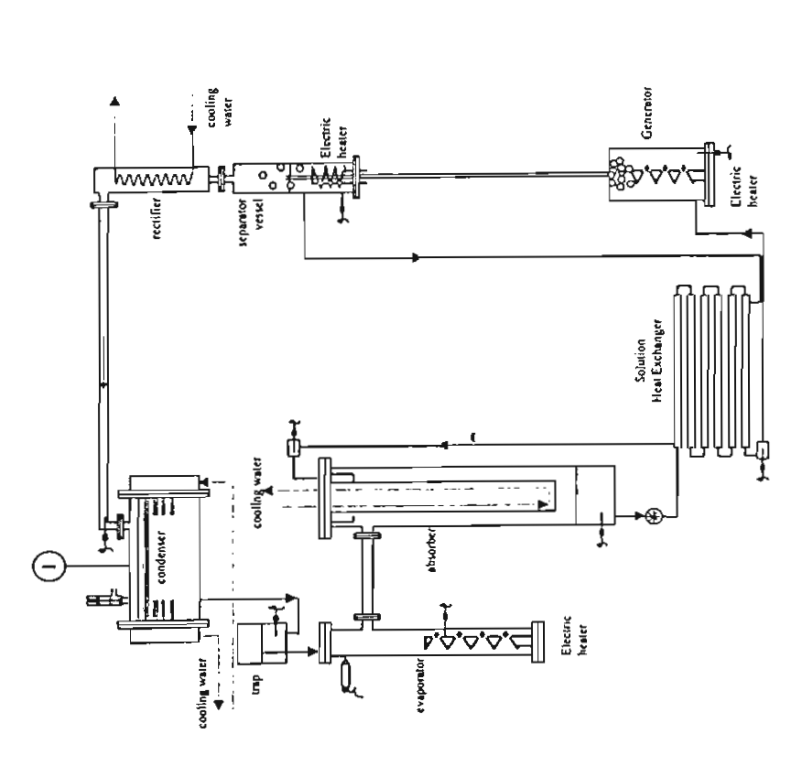


Figure A.2 The second configuration of the experimental DAR.

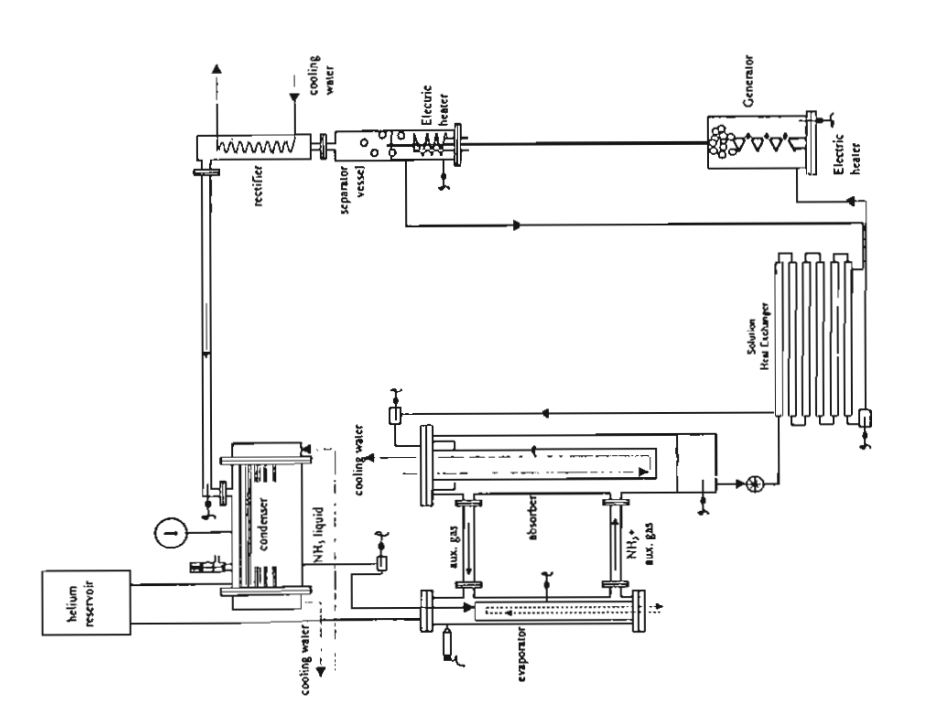


Figure A.3 The third configuration of the experimental DAR.

Figure A.4 The fourth configuration of the experimental DAR.

2. The second configuration

In the first design, coolness occurred at the trap tank. This was an undesirable phenomenon, as coolness should appear at the evaporator not at the trap tank. Moreover, it should take time for liquid ammonia to have enough volume that could flow down to the evaporator. As the liquid refrigerant in the trap tank was slowly increased therefore, the trap tank was removed. Knowing later that evaporation of liquid ammonia in the DAR is similar to evaporation of water from wet cloth and is definitely different from evaporation due to boiling of liquid. Therefore, evaporation of liquid ammonia in the DAR requires good mass transfer mechanisms. It requires evaporation surface area, period of absorption, different concentration, and flowing velocity of the auxiliary gas. To improve gas circulation in the system, an additional pipe connecting the evaporator and the absorber was installed around 10cm higher than the bottom of the evaporator horizontally to the absorber.

The evaporated ammonia mixes with the auxiliary gas and becomes heavier. It flows downward in the evaporator passing through the lower pipe into the absorber. In the absorber, ammonia vapor is absorbed by the strong solution flowing down as falling film. After the ammonia vapor was absorbed, the auxiliary gas became relatively lighter. Then, it flows upward to the top of absorber and flows back through the higher pipe into the evaporator. The gas circulation is established and mass transfer mechanisms can be enhanced.

With this design configuration, the liquid refrigerant cannot be accumulated in the evaporator. Therefore, the electric heater inside the evaporator was taken out. If there is liquid refrigerant accumulated, it will flow through the lower pipe into the absorber. So, cooling effect should be quantified by a different manner.

A 2in-pipe column was inserted vertically into the evaporator instead of the electric heater. There was an arrangement of flowing path for water circulation inside the pipe. Cooling effect from evaporation of ammonia in the evaporator would transfer to the water circulating inside the pipe. External surface of the inserted pipe were grooved to increase flowing period of the liquid refrigerant.

Referring to figure A.2, there was a tank installed at the top of the test rig. It was used as a helium storage tank. At the bottom, there were two small pipes connected. One was connected to the elbow pipe above the condenser, the other was connected to the top of the evaporator. These two tubes were used as pressure equalizing tubes between evaporator-absorber and the condenser. With these tubes, flowing of liquid refrigerant could be continued as a result of difference in the elevation. The trap tank was removed and a u-tube was installed as a trap between the condenser and the evaporator instead. It was used to prevent flowing of helium from the evaporator into the condenser during the operation

With this design configuration, a cooling effect occurred at the evaporator. There was ice formed at the outer surface of the evaporator after being operated for a while. The lower pipe connecting the evaporator and absorber was cool while the other was warm. It could be ensured that there must be circulation of the working fluid in these two pipes. Helium after absorption process flowed through the higher one. This could be implied from warming of the higher pipe as a result of absorption heat coming up with helium. Evaporated ammonia and helium flowed through the lower one. It could be implied from coolness appearing at the lower pipe. Cooling effect occurred in the evaporator due to evaporation of liquid ammonia.

It was noticed that the ammonia was not completely evaporated. The unevaporated ammonia was passed into the absorber together with evaporated ammonia and helium. For

a few hours of operation, a pressure-equalizing tube connected to the evaporator was warm. It was found that heat was transferred from the helium reservoir. It was traced further and found that heat was transferred from the elbow pipe above the condenser. As there was a flow of rectified vapor from the rectifier through this pipe into the condenser. Heat coming up with the rectified vapor was transferred to the helium reservoir. It was transferred further into the evaporator through the pressure equalizing tube. This was an undesired effect, as it became an additional heat load for the evaporator.

3. The third configuration

According to the prior design configuration, unwanted internal heat was transferred to the evaporator. The heat originated from the rectified refrigerant vapor leaving the rectifier. It was transferred through a pressure equalizing tube connected at the elbow pipe above the condenser. Therefore, the end of this tube that was connected to the elbow pipe was moved. Its connected position was moved to the top of condenser instead. Knowing that condensation temperature of the refrigerant vapor in the condenser was maintained by cooling water temperature. Its temperature was certainly lower than that at the elbow pipe.

With this design configuration, the system was found to work properly. However, heat transfer through the column pipe inserted inside the evaporator was not adequate. Some liquid refrigerant flowed along the grooved column pipe and was spin out due to high velocity flow along the helix-grooved surface. Then, the liquid refrigerant was not totally evaporated on the external surface of the grooved pipe. This caused a reduction of the cooling capacity. Moreover, heat transfer between the evaporated refrigerant in the evaporator and water circulated inside the grooved pipe should be poor due to the thickness of the inserted pipe.

4. The fourth configuration

Due to poor heat transfer at the evaporator, the system configuration was focused on the mechanism of heat transfer in the evaporator. Cooling capacity that would be obtained from evaporation of liquid ammonia in the evaporator should be quantified. Therefore, an electric heater was installed to supply a quantified heat load for the refrigerant. It was known from the prior design that heat could not be supplied directly when the ammonia was being evaporated. Therefore, it was supplied to the liquid refrigerant before being evaporated. After the evaporation process, the temperature of the liquid refrigerant should be reduced by evaporation of liquid ammonia in the evaporator.

The cooling capacity could be quantified directly from the power of heat supply by the electric heater. To enhance the mass transfer, the grooved pipe was removed. Raschig rings; hollowed porcelain cylinders, were loaded into the evaporator column instead. These rings were used to retard flow of liquid refrigerant through the evaporator. Therefore, flow period of liquid refrigerant was prolonged. It extended the evaporation period and increased the evaporation surface area, which resulted in better evaporation rate of ammonia.

Refer to figure A.4, there was a small cap at bottom of the evaporator. It was used to accumulate the remaining liquid refrigerant after evaporation in the evaporator through the ceramic fills. This liquid was pumped via a diaphragm pump through a heat exchanger with an electric heater inside. Heat supply from the heater was directly transferred to the cooled liquid refrigerant. The amount of heat was measured by a power transducer connected via the data acquisition system. The heated liquid refrigerant was pumped and sprayed into the evaporator at the top over the fills. It was then evaporated reducing refrigerant temperature while flowing downward over the fills.

However, during the test, the diaphragm pump leaked as one of its rubber diaphragms was torn. Therefore, this design configuration has not completely operated yet. It was considered that the diaphragm might be torn by cracked parts of raschig rings. The cracked ceramics were hard and had sharp edges, which could damage the rubber diaphragm. Therefore, it might not be convenient to include the diaphragm pump into the system. Moreover, the pump parts had to be imported, which required some period of delivery time. If it was damaged again, it would not be convenient.

5. The fifth configuration

In the fourth configuration, the cooling effect extraction procedure was done by use of an electric heater. However, there was leakage of the diaphragm pump. Another problem was the bubble pump performance, which was discovered later during the system commissioning.

During the tests, input heat at the generator was varied. It was once abruptly increased from low to high power in order to observe the system response. It was found that after sudden increment of input power at the generator, the solution was stopped flowing for a while. It could be seen by observation through sight glasses at the absorber. It was noticed that temperature at top of the generator was rather high comparing to that before abrupt heating. During the system disassembly, it was found that the heater in the generator was burnt. Burnt surface was noticed at the higher end of the heater.

The heater might be exposed to the gas, which was generated and accumulated at the top portion of the generator. Knowing that vapor phase, has lower heat capacity than that of liquid phase, if heat dissipated from the heater was too high to be transferred out properly, the heater would burn by its exceeding power. A sudden increment of heat input tended to cause intermittent pumping effect of the bubble pump. Then, the generator was

reconfigured in order to solve this problem. From the first 4 design configurations, the generator was erected as shown schematically in figure A.1 to A.4. In this design configuration, the generator was laid horizontally and fixed at the lowest level of the set-up as possible so as to maximize the head ratio as much as possible. In the generator, the pump tube configuration was rearranged. A tube was used for vaporized solution to flow. One of its ends was connected to the side of the generator, the other end was connected to the other tube at a t-connector. The second tube was used as a path for liquid solution to flow in. By this configuration, the bubble pump could be operated continuously.

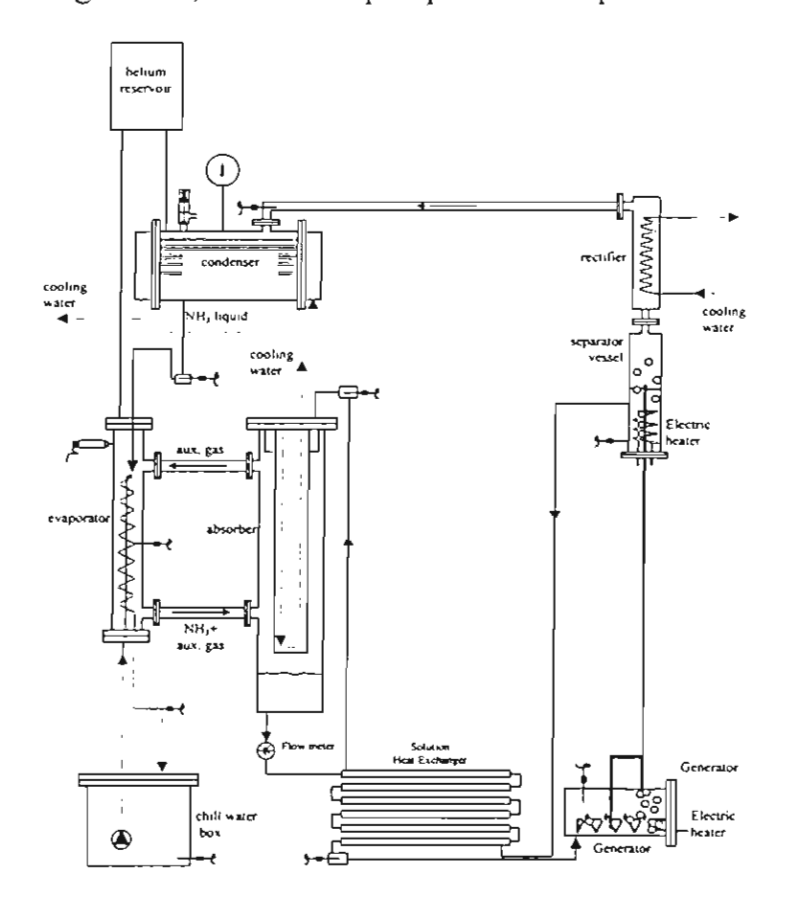


Figure A.5 The fifth configuration of the experimental DAR.

Due to exclusion of the diaphragm pump at the evaporator, transfer of the cooling effect was altered. A water chiller was installed instead of ceramic fills. In the evaporator, a 3/8in tube of 6m long was coiled and put inside the evaporator. Fresh water was circulated inside the coiled tube so as to be chilled by evaporation of refrigerant at the

outer tube surface. To circulate the chilled water, a small aquarium pump was put into the chilled water box. The chilled water was stored in an well-insulated icebox so as to prevent unwanted heat gain from the surroundings.

This design was the final version, which already described in chapter 3. All the tested results discussed throughout this thesis were obtained from this final design.

APPENDIX B

Calculation functions of selected thermodynamics properties of the ammonia-water system

A set of equations for calculation of ammonia-water solution properties used in the study was obtained from Patek and Klomfar [1995]. Five functions for calculations of the selected properties are,

$$T(p,x) = T_0 \sum_{i} a_i (1-x)^{m_i} \left[\ln \left(\frac{P_0}{p} \right) \right]^{n_i}$$
 (b-1)

$$T(p, y) = T_0 \sum_{i} a_i (1 - y)^{m_i - 4} \left[\ln \left(\frac{p_0}{p} \right) \right]^{n_i}$$
 (b-2)

$$y(p,x) = 1 - \exp\left[\ln(1-x)\sum_{i} a_{i} \left(\frac{p}{p_{0}}\right)^{m_{i}} x^{n_{i}/3}\right]$$
 (b-3)

$$h_i(T, x) = h_0 \sum_i a_i \left(\frac{T}{T_0} - 1\right)^{m_i} x^{n_i}$$
 (b-4)

$$h_{g}(T, y) = h_{0} \sum_{i} a_{i} \left(1 - \frac{T}{T_{0}}\right)^{m_{i}} (1 - y)^{n_{i}/4}$$
 (b-5)

Coefficients and exponents for function specified in equation (b-1) to (b-5) are listed in table b.1 to table b.5 respectively. In the calculations, these functions are used to calculate in reverse manner e.g. concentration of liquid, x, could be calculated with the specified T and p by iteration of equation (b-1). However, concentrations are specified in mole fraction, which could be converted into mass basis by,

$$w = \frac{yM_A}{vM_A + (1-v)M_w} \tag{b-6}$$

Table B.1 $T_0 \approx 100 \text{K}$ $p_0 = 2 \text{MPa}$

Table B.3 p₀=2MPa

i	m	n.	
1	0	0	$+0.322302 \times 10^{1}$
2	0	1	-0.384206×10^{0}
3	0	2	$+0.460965 \times 10^{-1}$
4	0	3	-0.378945 x 10 ⁻²
5	0	4	+0.135610x 10 ⁻³
6	1	0	$+0.487755 \times 10^{0}$
7	Ī	1	-0.120108×10^{9}
8	1	2	$+0.106154 \times 10^{-1}$
9	2	3	-0.533589×10^{-3}
10	4	0	$+0.785041 \times 10^{1}$
11	5	0	-0.115941×10^{2}
12	5	1	-0.523159 x 10 ⁻¹
13	6	0	$+0.489596 \times 10^{1}$
14	13	1	$+0.421059 \times 10^{-1}$

i	m,	n.	a,
1	0	0	$+1.98022017 \times 10^{1}$
2	0	1	$-1.18092669 \times 10^{1}$
3	0	6	$\pm 2.77479980 \times 10^{1}$
4	0	7	-2.88634277 x 10 ¹
5	l	0	-5.91616608 x 10 ¹
6	2	1	$+5.78991305 \times 10^{2}$
7	2	2	-6.21736743 x 10 ^e
8	3	2	-3.42198402×10^3
9	4	3	$+1.19403127 \times 10^4$
10	5	4	-2.45413777×10^4
11	6	5	$+2.91591865 \times 10^{4}$
12	7	6	-1.84782290 x 10 ⁴
13	7	7	$+2.34819434 \times 10^{1}$
14	8	7	$+4.80310617 \times 10^{3}$

Table B.2 $T_0=100K$ $p_0=2MPa$

Table B.4 $T_0=273.16 \, \mathrm{K} / h_0=100 \, \mathrm{kJ \cdot kg^{-1}}$

$\begin{array}{cccccccccccccccccccccccccccccccccccc$				
2 0 1 -0.395920 x 10 ⁰ 3 0 2 +0.435624 x 10 ⁻¹ 4 0 3 -0.218943 x 10 ⁻² 5 1 0 -0.143526x 10 ¹ 6 1 1 +0.105256 x 10 ¹ 7 1 2 -0.719281 x 10 ⁻¹ 8 2 0 +0.122362 x 10 ² 9 2 1 -0.224368 x 10 ¹ 10 3 0 -0.201780 x 10 ² 11 3 1 +0.110834 x 10 ¹ 12 4 0 +0.145399 x 10 ² 13 4 2 +0.644312 x 10 ⁰ 14 5 0 -0.221246 x 10 ¹ 15 5 2 -0.756266 x 10 ⁰ 16 6 0 -0.135529 x 10 ¹	i	m	n.	
3 0 2 +0.435624 x 10 ⁻¹ 4 0 3 -0.218943 x 10 ⁻² 5 1 0 -0.143526x 10 ¹ 6 1 1 +0.105256 x 10 ¹ 7 1 2 -0.719281 x 10 ⁻¹ 8 2 0 +0.122362 x 10 ² 9 2 1 -0.224368 x 10 ¹ 10 3 0 -0.201780 x 10 ² 11 3 1 +0.110834 x 10 ¹ 12 4 0 +0.145399 x 10 ² 13 4 2 +0.644312 x 10 ⁰ 14 5 0 -0.221246 x 10 ¹ 15 5 2 -0.756266 x 10 ⁰ 16 6 0 -0.135529 x 10 ¹	1	0	0	$+0.324004 \times 10^{1}$
4 0 3 -0.218943 x 10 ⁻² 5 1 0 -0.143526x 10 ¹ 6 1 1 +0.105256 x 10 ¹ 7 1 2 -0.719281 x 10 ⁻¹ 8 2 0 +0.122362 x 10 ² 9 2 1 -0.224368 x 10 ¹ 10 3 0 -0.201780 x 10 ² 11 3 1 +0.110834 x 10 ¹ 12 4 0 +0.145399 x 10 ² 13 4 2 +0.644312 x 10 ⁰ 14 5 0 -0.221246 x 10 ¹ 15 5 2 -0.756266 x 10 ⁰ 16 6 0 -0.135529 x 10 ¹	2	0	1	-0.395920×10^{0}
5 1 0 -0.143526x 10 ¹ 6 1 1 +0.105256 x 10 ¹ 7 1 2 -0.719281 x 10 ⁻¹ 8 2 0 +0.122362 x 10 ² 9 2 1 -0.224368 x 10 ¹ 10 3 0 -0.201780 x 10 ² 11 3 1 +0.110834 x 10 ¹ 12 4 0 +0.145399 x 10 ² 13 4 2 +0.644312 x 10 ⁰ 14 5 0 -0.221246 x 10 ¹ 15 5 2 -0.756266 x 10 ⁰ 16 6 0 -0.135529 x 10 ¹	3	0	2	$+0.435624 \times 10^{-1}$
6 1 1 +0.105256 x 10 ¹ 7 1 2 -0.719281 x 10 ⁻¹ 8 2 0 +0.122362 x 10 ² 9 2 1 -0.224368 x 10 ¹ 10 3 0 -0.201780 x 10 ² 11 3 1 +0.110834 x 10 ¹ 12 4 0 +0.145399 x 10 ² 13 4 2 +0.644312 x 10 ⁰ 14 5 0 -0.221246 x 10 ¹ 15 5 2 -0.756266 x 10 ⁰ 16 6 0 -0.135529 x 10 ¹	4	0	3	-0.218943 x 10 ⁻²
7 1 2 -0.719281 x 10 ⁻¹ 8 2 0 +0.122362 x 10 ² 9 2 1 -0.224368 x 10 ¹ 10 3 0 -0.201780 x 10 ² 11 3 1 +0.110834 x 10 ¹ 12 4 0 +0.145399 x 10 ² 13 4 2 +0.644312 x 10 ⁰ 14 5 0 -0.221246 x 10 ¹ 15 5 2 -0.756266 x 10 ⁰ 16 6 0 -0.135529 x 10 ¹	5	1	0	-0.143526x 10 ¹
8 2 0 +0.122362 x 10 ² 9 2 1 -0.224368 x 10 ¹ 10 3 0 -0.201780 x 10 ² 11 3 1 +0.110834 x 10 ¹ 12 4 0 +0.145399 x 10 ² 13 4 2 +0.644312 x 10 ⁰ 14 5 0 -0.221246 x 10 ¹ 15 5 2 -0.756266 x 10 ⁰ 16 6 0 -0.135529 x 10 ¹	6	1	1	$+0.105256 \times 10^{1}$
9 2 1 -0.224368 x10 ¹ 10 3 0 -0.201780 x 10 ² 11 3 1 +0.110834 x 10 ¹ 12 4 0 +0.145399 x 10 ² 13 4 2 +0.644312 x 10 ⁰ 14 5 0 -0.221246 x 10 ¹ 15 5 2 -0.756266 x 10 ⁰ 16 6 0 -0.135529 x 10 ¹	7	1	2	-0.719281×10^{-1}
10 3 0 -0.201780 x 10 ² 11 3 1 +0.110834 x 10 ¹ 12 4 0 +0.145399 x 10 ² 13 4 2 +0.644312 x 10 ⁰ 14 5 0 -0.221246 x 10 ¹ 15 5 2 -0.756266 x 10 ⁰ 16 6 0 -0.135529 x 10 ¹	8	2	0	$+0.122362 \times 10^{2}$
11 3 1 +0.110834 x 10 ¹ 12 4 0 +0.145399 x 10 ² 13 4 2 +0.644312 x 10 ⁰ 14 5 0 -0.221246 x 10 ¹ 15 5 2 -0.756266 x 10 ⁰ 16 6 0 -0.135529 x 10 ¹	9	2	1	-0.224368 x10 ¹
12 4 0 +0.145399 x 10 ² 13 4 2 +0.644312 x 10 ⁰ 14 5 0 -0.221246 x 10 ¹ 15 5 2 -0.756266 x 10 ⁰ 16 6 0 -0.135529 x 10 ¹	10	3	0	-0.201780×10^{2}
13 4 2 +0.644312 x 10 ⁰ 14 5 0 -0.221246 x 10 ¹ 15 5 2 -0.756266 x 10 ⁰ 16 6 0 -0.135529 x 10 ¹	11	3	1	$+0.110834 \times 10^{1}$
14 5 0 -0.221246 x 10 ¹ 15 5 2 -0.756266 x 10 ⁰ 16 6 0 -0.135529 x 10 ¹	12	4	0	$+0.145399 \times 10^{2}$
15 5 2 -0.756266 x 10° 16 6 0 -0.135529 x 10°	13	4	2	$+0.644312 \times 10^{0}$
16 6 0 -0.135529×10^{1}	14	5	0	-0.221246×10^{1}
	15	5	2	-0.756266×10^{0}
17 7 2 $\pm 0.183541 \times 10^{\circ}$	16	6	0	-0.135529×10^{1}
	1.7	7	2	$+0.183541 \times 10^{0}$

i	m_i	n _i	a,
1	0	0	-0.761080×10^{1}
2	0	1	$+0.256905 \times 10^{2}$
3	0	6	-0.247092×10^3
4	0	7	$+0.325952 \times 10^{3}$
5	0	0	-0.158854×10^3
6	0	1	$+0.619084 \times 10^{2}$
7	1	2	$+0.114314 \times 10^{2}$
8	1	2	$+0.118157 \times 10^{1}$
9	2	3	$+0.284179 \times 10^{1}$
10	3	4	$+0.741609 \times 10^{1}$
11	5	5	$\pm 0.891844 \times 10^{3}$
12	5	5	-0.161309×10^4
13	5	5	$+0.622106 \times 10^{3}$
14	6	6	-0.207588×10^{3}
15	6	7	-0.687393×10^{1}
16	8	7	$+0.350716 \times 10^{1}$

Table B.5 $T_0=324K h_0=1000kJ\cdot kg^{-1}$

ii	m,	n,	a,
1	0	0	$+0.128827 \times 10^{1}$
2	ì	0	$+0.125247 \times 10^{0}$
3	2	0	-0.208748×10^{1}
4	3	0	-0.217696×10^{1}
5	0	2	$+0.235687 \times 10^{1}$
6	1	2	-0.886987×10^{1}
7	2	2	$+0.102635 \times 10^{2}$
8	3	2	-0.237440×10^{1}
9	0	3	-0.670515×10^{1}
10	1	3	$+0.164508 \times 10^{2}$
I 1	2	3	-0.936849 x 10 ¹
12	0	‡	$\pm 0.842254 \times 10^{1}$
13	1	4	-0.858807×10^{1}
14	0	5	-0.277049×10^{1}
15	-\$	6	-0.961248×10^{0}
16	2	7	$+0.988009 \times 10^{0}$
1.7	1	10	$+0.308482 \times 10^{0}$

Nomenclature

h enthalpy (kJ kg⁻¹)

M Molar mass (kg kmol⁻¹)

p Pressure (M Pa)

T Temperature (K)

x Ammonia mole fraction in liquid phase
y Ammonia mole fraction in gas phase
w Ammonia mass fraction in gas phase

Subscripts

A Ammonia
g Gas phase
i term of fitting polynomial
Liquid phase
W Water

0 Reference value

APPENDIX C

A Calculation Example of The Mathematical Model

An example of the calculation of the proposed mathematical model is shown with selected operating conditions. Its operating conditions are shown in table C.1. The calculated properties were based on locations specified in figure 5.1.

Table C.1 Operating condition of the calculation example.

Helium charge pressure	6.1bar
Operating pressure	13.2bar
Solution concentration	0.23
Heat input	1.3kW
Rectification temperature	73.3°C
Cooling water temperature	31.8°C
Generator temperature	137.4°C
Solution temperature at generator inlet	109.2°C

At the operating pressure of 13.2bar and solution temperature in the generator of 137.4°C, which was considered as saturated state, its vapor concentration could be calculated as [Patek and Klomfar, 1995], $x_4 = 0.762$ and the concentration of liquid phase was, $x_3 = 0.198$. Thus, the calculated enthalpy of both vapor and liquid phase were as follows,

$$h_4 = 1,819.2 \text{ kJ} \cdot \text{kg}^{-1}$$

$$h_3 = 453.5 \text{ kJ} \cdot \text{kg}^{-1}$$

The specific volume of the liquid as well as vapor solution could be calculated by equation (5.6) and (5.7) respectively,

$$\upsilon_{3} = (1-X_{3})~\upsilon_{water-liq} + 0.85~X_{3}~\upsilon_{amm-liq}$$
 ,

properties in this equation were based on the operating temperature of the generator (saturated at temperature).

$$\upsilon_4 = (1 - X_4) \upsilon_{water-vap} + X_4 \upsilon_{amm-vap}$$

properties in the prior equation were based on the operating pressure (saturated at pressure). The calculated $v_3 = 0.00158 \text{ m}^3 \cdot \text{kg}^{-1}$ and $v_4 = 0.00158 \text{ m}^3 \cdot \text{kg}^{-1}$.

Enthalpy of the liquid solution at the generator inlet, with x = 0.23, was calculated as, $h_1 = 308.2 \text{ kJ}\cdot\text{kg}^{-1}$. These values were substituted into equation (5.1) with $\dot{Q}_{in} = 1.3 \text{kW}$. It was solved and the obtained volume flow rate of the vaporized solution was obtained as,

$$\dot{V}_4 = 2.184 \, l \, min^{-1}$$
.

It could be converted into mass flow rate by using specific volume v4 as,

$$\dot{m}_4 = 0.3303 \text{ g} \cdot \text{s}^{-1}$$

Mass flow rate of the pumped liquid could be obtained as,

$$\dot{m}_3 = 5.5118 \text{ g} \cdot \text{s}^{-1}$$

At this stage, the concentration was balanced by equation (5.8),

$$\dot{m}_1 x_1 = \dot{m}_3 x_3 + \dot{m}_4 x_4$$

If the value of x_1 was not valid, $x_1 \neq 0.23$, the calculation steps must be repeated with corrected x_1 . However, in this calculation, the obtained balance was valid. Then, all obtained figures could be used for further calculations.

At the rectifier, the operating temperature was 73.3°C which could partially condense water vapor from the vaporized solution. The rectified vapor left the rectifier with concentration of, $x_7 = 0.984$. While the condensate that was partially condensed having concentration of, $x_5 = 0.505$. Enthalpies of both streams were calculated as,

$$h_7 = 1,421.6 \text{ kJ} \cdot \text{kg}^{-1}$$

$$h_5 = 83.2 \text{ kJ} \cdot \text{kg}^{-1}$$

Mass flow rate of the rectified vapor (7) could be calculated from equation (5.9),

$$\dot{m}_7 = \frac{(x_6 - x_5)}{(x_7 - x_5)} \dot{m}_4 = 0.1771 \text{ g·s}^{-1}$$

and the condensate that was partially condensed was calculated as,

$$\dot{m}_5 = 0.1532 \text{ g} \cdot \text{s}^{-1}$$
.

The pumped liquid (3) and condensate (5) were mixed as the strong solution (9). The concentration of the strong solution, x_9 , could be calculated from equation (5.12),

$$x_9 = \frac{\dot{m}_3 x_3 + \dot{m}_5 x_5}{\dot{m}_3 + \dot{m}_5} = 0.206.$$

The rectified refrigerant vapor (7) was liquefied as liquid refrigerant (8) with mass flow rate, $\dot{m}_8 = \dot{m}_7$, and concentration, $x_8 = x_7$. Ammonia in the liquid solution was absorbed causing refrigerating effect in the evaporator. It was assumed that all of the obtained ammonia in the liquid refrigerant could be evaporated. Then its cooling capacity could be calculated from equation (5.14)

$$\dot{Q}_{evap} = \dot{m}_8 x_8 (h_{12-vap} - h_8)$$

Enthalpy of the evaporated ammonia in the evaporator could be calculated as,

$$h_{12\text{-vap}} = 1264.9 \text{ kJ} \cdot \text{kg}^{-1}$$

and the liquid refrigerant (8) enthalpy was calculated as $h_8 = 134.2 \text{ kJ} \cdot \text{kg}^{-1}$. Then the obtained cooling effect was calculated as,

$$\dot{Q}_{evap} = 196.7 \text{ W}.$$

When the absorption capability dropped, the combined evaporator-absorber effectiveness, ε , was included into consideration. It was defined as equation 5.18 as,

$$\varepsilon = \frac{\dot{m}_{11} x_{11} - \dot{m}_{10} x_{10}}{\dot{m}_8 x_8}$$

The effectiveness was varied from 1 down to 0.5 with a step of 0.1. In this example, it was assumed to be 0.7. With less absorption capability, the cooling effect was decreased as a result of less evaporated ammonia. Then the obtained cooling capacity could be estimated as,

$$\dot{Q}_{evap} = 154.3 \text{ W}.$$

Concentration of liquid refrigerant that was left in the evaporator could be calculated as,

$$x_{12}$$
" = 0.949

With mass flow rate of,

$$\dot{m}_{12} = 0.0551 \text{ g·s}^{-1}$$

The concentration of the weak solution after absorption process (13) should be checked to verify the obtained results. Then, it was calculated by equation (5.23) as,

$$x_{13} = 0.2299 \cong 0.23$$

The calculated results are listed in table C2.

Table C2 Calculated results $\epsilon = 1.0$

ε – 1.0					
location	T (°C)	Х	h (kJ·kg ⁻¹)	m (g·sʾ	¹) phase
1	109.7	0.229	308.2	5.842	liquid
2	137.4	0.229	530.7	5.842	mixture
3	137.4	0.198	453.5	5.512	sat liquid
4	137.4	0.762	1819.2	0.330	sat vapor
5	73.3	0.505	83.2	0.153	sat liquid
6	73.3	0.762	800.9	0.330	mixture
7	73.3	0.984	1421.6	0.177	sat vapor
8	31.8	0.984	134.2	0.177	liquid
9	136.0	0.206	443.5	5.665	liquid
10	68.5	0.206	138	5.665	liquid
11	43.0	0.229	11.8	5.839	liquid
12 liq	0.0	0.000	-0.04	0.003	liquid
12 vap	0.0	1.000	1264.9	0.174	vapor
13	43.0	0.229	11.8	5.842	liquid
,					
07					
$\varepsilon = 0.7$					•••••
11	43.0	0.223	11.8	5.787	liquid
12 liq	0.0	0.949	-0.04	0.055	liquid
12 vap	0.0	1.000	1264.9	0.122	vapor
13	43.0	0.229	11.8	5.842	liquid

APPENDIX D

Test Results

D.1 Variation of the generator heat input

Table D.1 Helium charge pressure 6.1bar

Input kW	MPa	7	8	2	1	13	3	Cooling effect	COP
1	1.236	72.24	31.45	135.21	105.59	36.71	132.87	67.60	0.0942
1.1	1.251	72.48	31.42	135.73	106.27	37.25	133.61	92.86	0.1110
1.2	1.321	73.15	31.63	139.39	109.91	43.46	137.30	120.50	0.1273
1.3	1.318	73.34	31.77	139.14	109.14	43.07	137.35	131.82	0.1273
1.5	1.274	73.21	31.66	136.26	104.70	39.07	134.95	132.79	0.1110
1.75	1.268	73.39	31.24	136.07	103.65	39.61	135.04	132.54	0.0950
2	1.312	74.76	31.87	138.98	107.41	44.50	138.54	158.33	0.0974
2.25	1.340	75.86	31.56	140.50	109.66	46.66	141.35	188.44	0.1014
2.5	1.275	74.47	31.33	136.87	101.53	41.79	135.58	167.53	0.0820

Table D.2 Helium charge pressure 6.8bar

Input kW	MPa	7	8	2	1	13	3	Cooling effect	COP
1.0	14.103	72.48	32.16	142.00	112.16	41.61	140.19	96.56	0.126
1.1	13.601	72.43	31.64	139.53	109.48	37.67	137.37	126.96	0.145
1.2	13.742	72.46	31.92	139.80	108.64	38.05	138.12	126.22	0.133
1.3	13.745	73.17	32.95	141.28	109.72	42.78	139.64	162.19	0.153
1.4	13.767	73.84	32.53	140.89	110.07	42.46	139.64	147.82	0.131
1.5	13.741	73.37	32.31	139.83	108.08	40.26	138.86	156.17	0.128
1.75	14.022	74.89	32.13	141.72	110.32	44.64	141.05	149.07	0.105
2.0	13.729	75.29	30.95	141.09	109.23	44.55	140.89	161.70	0.099
2.25	14.056	76.05	31.38	142.88	111.35	46.85	143.58	182.96	0.099
2.5	13.535	75.62	32.28	140.80	105.27	43.22	139.67	190.86	0.093

Table D.3 Helium charge pressure 8.2bar

Input kW	MPa	7	8	2	1 (13	3	Cooling effect	COP
1.5	1.439	74.41	32.01	142.22	111.26	41.31	142.27	192.21	0.165
1.75	1.438	75.20	32.23	142.45	109.94	42.11	142.15	196.10	0.144
2	1.440	75.34	32.35	142.71	108.80	42.37	142.02	181.40	0.117
2.25	1.425	75.64	32.19	142.33	107.01	42.67	141.10	181.47	0.104
2.5	1.437	75.76	32.07	142.88	107.21	43.38	142.05	199.49	0.102

Table D.4 Helium charge pressure 9.5bar

Input kW	MPa	7	8	2	1	13	3	Cooling effect	COP
1.75	16.083	70.13	32.16	114.78	146.67	44.24	146.66	154.96	0.109
2	15.542	75.54	31.81	112.56	145.03	43.69	145.89	182.92	0.111
2.1	15.348	75.39	31.37	110.27	144.53	43.20	144.59	163.11	0.095
2.25	15.890	76.16	31.65	114.34	147.38	45.74	148.16	193.30	0.104
2.4	15.742	76.36	31.96	113.16	147.28	45.75	147.44	209.92	0.126
2.5	15.577	76.07	31.73	111.23	146.22	45.03	146.28	218.46	0.132
2.6	16.028	77.03	31.71	116.43	150.55	47.90	151.28	241.72	0.113

D.2 Variation of rectification temperature

Table D.5 Helium charge pressure 6.1 bar

Rect. temp	MPa	7	8	2	1	13	3	Cooling effect	COP
50-55	1.246	51.75	31.87	135.78	103.34	39.97	134.39	122.71	0.089
55-60	1.276	56.63	31.60	137.85	106.47	43.49	136.63	137.59	0.098
60-65	1.267	61.48	30.21	137.57	105.96	43.27	136.44	140.76	0:100
65-70	1.289	66.09	31.69	138.48	107.21	44.67	137.35	125.08	0.090
70-75	1.245	70.21	31.71	136.14	103.64	40.39	134.72	125.47	0.090
75-80	1.268	73.39	31.24	136.07	103.65	39.61	135.04	132.54	0.095
80-85	1.248	77.67	31.34	135.58	102.74	40.01	134.47	118.30	0.086
85-90	1.245	82.31	31.23	135.55.	102.83	40.20	134.50	115.33	0.084

Table D.6 Helium charge pressure 6.8bar

Rect.	MPa	7	8	2	1	13	3	Cooling effect	COP
50-55	13.274	52.01	31.56	138.73	105.94	40.47	137.66	171.10	0.119
55-60	13.676	56.67	31.48	140.82	109.59	44.40	140.15	139.66	0.099
60-65	13.593	61.56	31.71	140.65	109.15	44.61	139.91	144.92	0.103
65-70	13.439	66.24	31.35	140.05	108.64	43.64	139.25	145.92	0.103
70-75	13.017	70.28	31.32	137.68	104.98	40.07	136.75	153.40	0.108
75-80	14.022	74.89	32.13	141.72	110.32	44.64	141.05	149.07	0.105
80-85	13.040	78.21	31.50	138.15	105.58	40.22	137.18	150.84	0.107
85-90	13.401	82.83	30.92	139.89	108.66	44.31	139.43	142.07	0.101
90-95	12.978	87.00	31.39	137.53	105.02	39.89	136.41	137.32	0.098

Table D.7 Helium charge pressure 8.2bar

Rect.	MPa	7	8	2	1	13	3	cooling effect	COP
50-55	1.416	51.73	32.06	141.71	108.1526	40.96	140.772	174.15	0.121
55-60	1.443	56.75	31.64	143.51	111.51	44.56	143.19	153.93	0.109
60-65	1.404	61.50	31.03	141.54	109.25	42.25	140.99	164.69	0.115
65-70	1.377	65.99	31.33	140.43	107.24	40.30	139.38	176.85	0.123
70-75	1.368	70.51	30.81	139.71	106.74	39.91	138.79	175.19	0.122
75-80	1.438	75.20	32.24	142.46	109.95	42.12	142.16	196.11	0.135
80-85	1.409	79.36	31.34	141.93	109.99	43.82	141.15	153.52	0.108
85-90	1.358	82.18	30.92	139.15	106.00	39.56	138.20	166.30	0.116
90-95	1.433	86.63	31.97	142.02	108.99	41.08	141.12	157.43	0.111